Fermi National Accelerator Laboratory

FERMILAB-FN-655

# "Round Colliding Beams" As a Way to Integrability: Theory and Simulations for Tevatron

V.V. Danilov and V.D. Shiltsev

*Fermi National Accelerator Laboratory*
*P.O. Box 500, Batavia, Illinois 60510*

February 1997

Operated by Universities Research Association Inc. under Contract No. DE-AC02-76CH03000 with the United States Department of Energy

## Disclaimer



## Distribution

# "Round Colliding Beams" As a Way to Integrability: Theory and Simulations for Tevatron

V.V. Danilov*, V.D. Shiltsev

*Fermi National Accelerator Laboratory*

*P.O. Box 500, Batavia, Illinois 60510*

February 21, 1997

**Abstract**

This paper presents investigation of the proposed use of round beams for increasing a luminosity in colliders. The main idea of round beams is in existing integral of motion: angular momentum. It is shown in this paper, that it's possible to construct systems with colliding beams with one additional integral of motion, so these systems are integrable in classical(Liouville) sense and particle's motion is regular. Among the examples of integrable systems with round beams there is one with a soliton-like solution for the interaction force. We also show how the general theory of integrable systems relates to our subject. Numerical simulations of round colliding beams for the Tevatron are much in favor of round beams, because they provide reduction of harmful impact of beam-beam forces on beam sizes, particles diffusion and better stability with respect to errors and imperfections.

*Permanent address: Budker Institute of Nuclear Physics, 630090, Novosibirsk, Russia

# Contents

# 1 Introduction

The concept of "round colliding beams" (RCBs) is considered as a possibility to reach higher luminosity and to improve beam stability in colliders for almost twenty years. The concept made a long way from the idea itself and early theoretical and numerical studies (see e.g. [1, 2, 3]), through extended studies of its application to electron-positron colliders (see e.g.[4, 5], J.Byrd, *et. al* in [6], [7, 8, 9, 10, 11], and, recently, the first experimental test of the round beams has been performed at CESR (see E.Young in [12]). The current status of the RCBs concept was surveyed at the Mini-Workshop on "Round Beams and Related Concepts in Beam Dynamics" (Fermilab, December 1996) [12].

Accordingly to Ref.[11] the essential conditions of the round beams are:

- equal horizontal and vertical emittances $\varepsilon_x = \varepsilon_y = \varepsilon$;
- equal horizontal and vertical beta-functions at interaction point (IP) $\beta_x^* = \beta_y^* = \beta^*$;
- equal horizontal and vertical tunes $\nu_x = \nu_y = \nu$.

Beam-beam interaction of two beams with Gaussian charge density profile is characterized by parameter of:

$$\xi_{x,y} = \frac{N r_0}{2\pi\gamma} \frac{\beta^*_{x,y}}{\sigma^*_{x,y}(\sigma^*_x + \sigma^*_y)}, \tag{1}$$

where $N$ is the number of particles in the opposite bunch, $r_0 = e^2/mc^2$ is the particles classical radius, $\gamma = E/mc^2$ is the relativistic factor, and $\sigma_{x,y}$ are the rms horizontal and vertical beam sizes. While the parameters are small, they are equal to the tune shifts due to the beam-beam interaction. In the case of not equal sizes, the kick due to the interaction depends on longitudinal position $s$ within the bunch, because generally speaking the beta-function is not constant $\beta_{x,y} = \beta_{x,y}(s)$. That leads to enhanced coupling between longitudinal and betatron motions, which disappears for round beams. Indeed, the beam-beam parameter for the round beams is equal to

$$\xi_{x,y} = \frac{N r_0}{4\pi\gamma\varepsilon}, \tag{2}$$

and does not depend on $s$ because the emittance $\varepsilon = \sigma^2/\beta$ is independent of the longitudinal coordinate.

Moreover, when all three conditions of the RCB are satisfied, the rotational symmetry of the kick from the round opposite beam, complemented with the $X - Y$ symmetry of the betatron transfer matrix between the collisions, result in an additional integral of motion $\mathcal{M} = xy' - yx'$ that is longitudinal component of the angular momentum. Thus, the transverse motion becomes equivalent to a one dimensional

(1D) motion. Resulting elimination of all betatron coupling resonances is of crucial importance, since they are believed to cause the beam-lifetime degradation and blow-up. The reduction to 1D motion makes impossible the diffusion through invariant circles [1]

The development of the instability due to the beam-beam interaction limits the maximum beam-beam parameter for flat beams in $e^+e^-$ colliders $\xi_F^{max} \lesssim 0.04$ while the RCBs simulation and the first experimental results dare to believe that the maximum parameter of $\xi_R^{max} \simeq 0.1$ can be easily achieved. Therefore, maximum luminosity of the collider:

$$L = \frac{f_0 B N^2}{4\pi\sigma_x^*\sigma_y^*} \propto I_{tot}\frac{\xi^{max}}{\beta^*}\frac{1+R}{2}, \tag{3}$$

can be increased about 5 times ($B$ denotes the number of bunches, $R = \sigma_y^*/\sigma_x^*$, $f_0$ is the frequency of collisions, we also assume here that total current $I_{tot}$ and $\beta^*$ are fixed due to other considerations).

It is not the case for hadron colliders where the beams are almost round from the beginning and the most useful predicted properties of the RCBs are their better stability, lower losses and longer beam lifetime, although some valuable increase in $\xi^{max}$ and in $L$ can be expected too.

In this article we present theoretical and numerical studies of the round beams. Section 2 of the paper is devoted to a general consideration of the angular momentum conserving matrix transformations and two practical examples for the round colliding beams are presented. The search for one-dimensional dynamical systems with invariants polynomial in momentum is performed in Section 3.The results of numerical simulations of round colliding beams in Tevatron collider are presented in Section 4 where the effects of various machine imperfections are considered. Section 5 summarizes the results and concludes the work.

# 2 Round Colliding Beams

There are variations in approaches of the cited above authors to attack the "round beams" effects, and in this paper we conceptually follow the work [11]. As we mentioned in the Introduction, the "round beams" require equal emittances and beta-functions at the interaction region and the conservation of the angular momentum in linear transformation in the arcs. Below, we find the general form of $4 \times 4$ matrices of a linear lattice, which preserves the angular momentum $\mathcal{M} = xy' - yx'$, where $x, y$ are the betatron displacements, and $x' = dx/ds$, $y' = dy/ds$ are their slopes.

[1] Indeed, the invariant line is the boundary of the inner space for periodic motion, then due to the fact that trajectories in the phase space can not intersect each other, so the motion from any point of the inner phase space through the boundary is not possible. For the 2D dynamics, such motion (so called Arnold diffusion) takes place, because the boundary in four-dimensional phase space has to have dimension of 3, while the invariant torus has only dimension of 2.

## 2.1 Linear matrices with angular momentum conservation

It's easy to understand, that all matrices of the form

$$R(\phi) \cdot \begin{pmatrix} T & 0 \\ 0 & T \end{pmatrix}$$

(where T is a $2 \times 2$ matrix with $detT = 1$ and R is the matrix of rotation over an angle $\phi$ ), have rotational symmetry and preserve the angular momentum. It's more complicated to prove, that there are no other matrices [2]. Here we follow the work [14].

Let's make the notation for vector of particle's coordinate and angle:

$$X = \begin{pmatrix} x \\ x' \\ y \\ y' \end{pmatrix};$$

here prime sign $'$ means derivative over "time" and "time" for simplicity everywhere in this paper means longitudinal coordinate $s$.

The angular momentum may be presented in the matrix form:

$$\mathcal{M} = \frac{1}{2} X^T \cdot L \cdot X, \tag{4}$$

here $^T$ means a transposed vector (or matrix) and

$$L = \begin{pmatrix} 0 & J \\ -J & 0 \end{pmatrix},$$

and J is $2 \times 2$ matrix

$$J = \begin{pmatrix} 0 & 1 \\ -1 & 0 \end{pmatrix}.$$

Let $M$ be a $4 \times 4$ matrix of the linear transformation which conserves the angular momentum for any $X$:

$$X^T \cdot M^T \cdot L \cdot M \cdot X = X^T \cdot L \cdot X, \tag{5}$$

or

$$M^T \cdot L \cdot M = L. \tag{6}$$

The matrix $M$ has to be symplectic, so we have

$$M^T \cdot S \cdot M = S, \tag{7}$$

[2] This was proved by E.Pozdeev [13]

where

$$S = \begin{pmatrix} J & 0 \\ 0 & J \end{pmatrix}.$$

From (6) one can obtain $M^T$, put it into in the previous equation (7), that yields

$$L \cdot S \cdot M = M \cdot L \cdot S, \tag{8}$$

$$L \cdot S = \begin{pmatrix} 0 & -I \\ I & 0 \end{pmatrix},$$

where $I$ is the $2 \times 2$ identity matrix.

We can rewrite previous equation after presenting $M$ in the block form:

$$M = \begin{pmatrix} A & B \\ C & D \end{pmatrix}$$

(here $A, B, C, D$ are $2 \times 2$ blocks), and rewrite (8):

$$\begin{pmatrix} -C & -D \\ A & B \end{pmatrix} = \begin{pmatrix} B & -A \\ D & -C \end{pmatrix}. \tag{9}$$

From there we have $A = D, B = -C$, or the angular momentum is conserved for all symplectic matrices

$$\begin{pmatrix} A & -C \\ C & A \end{pmatrix}. \tag{10}$$

The symplectic condition $S = M^T \cdot S \cdot M$ gives us relation between $A$ and $C$:

$$S = \begin{pmatrix} J & 0 \\ 0 & J \end{pmatrix} = M^T \cdot S \cdot M = \begin{pmatrix} A^T & C^T \\ -C^T & A^T \end{pmatrix} \begin{pmatrix} J & 0 \\ 0 & J \end{pmatrix} \begin{pmatrix} A & -C \\ C & A \end{pmatrix},$$

that results in:

$$A^T \cdot J \cdot A + C^T \cdot J \cdot C = J \tag{11}$$

$$A^T \cdot J \cdot C = C^T \cdot J \cdot A \tag{12}$$

For arbitrary matrix $A$ the equality $A^T \cdot J \cdot A = J \cdot detA$ is valid, then from (11) we get

$$detA + detC = 1. \tag{13}$$

Then, the condition (12) yields

$$J \cdot C \cdot A^{-1} = (C \cdot A^{-1})^T \cdot J.$$

From there one can get $C \cdot A^{-1} = I \cdot const$, or

$$C = A \cdot const. \tag{14}$$

Let us express $A$ and $C$ through matrix $T$ with $detT = 1$.

$$A = \alpha \cdot T, \quad C = -\beta \cdot T, \tag{15}$$

then from (13) we have

$$\alpha^2 + \beta^2 = 1.$$

Let $\alpha = \sin\phi$ and $\beta = \cos\phi$ ($\phi$ is an arbitrary angle), then one gets:

$$M = \begin{pmatrix} I \cdot \cos\phi & I \cdot \sin\phi \\ -I \cdot \sin\phi & I \cdot \cos\phi \end{pmatrix} \cdot \begin{pmatrix} T & 0 \\ 0 & T \end{pmatrix} = \begin{pmatrix} T \cdot \cos\phi & T \cdot \sin\phi \\ -T \cdot \sin\phi & T \cdot \cos\phi \end{pmatrix}. \tag{16}$$

Now $M$ is presented in the general form with only 4 arbitrary parameters (instead of 10 in general case of symplectic $4 \times 4$ matrix).

There is another interesting set of matrices $M$ which transform the sign of the angular momentum $\mathcal{M}$:

$$M = \begin{pmatrix} I \cdot \cos\phi & I \cdot \sin\phi \\ -I \cdot \sin\phi & I \cdot \cos\phi \end{pmatrix} \cdot \begin{pmatrix} T & 0 \\ 0 & -T \end{pmatrix}, \tag{17}$$

where $detT = 1$.

This case is also interesting for us, because the squared angular momentum $\mathcal{M}^{\in}$ is now invariant with respect to the linear transformation $M$ as well as the interaction with opposite round beam.

## 2.2 Next step to elimination of stochasticity: additional integral of motion

In the previous section we deal with 2D motion, which can be reduced to 1D motion due to the angular momentum conservation. But 1D motion with the time-dependent Hamiltonian, generally speaking, is also stochastic, although it has more "regularity" in comparison with a general 2D motion. What we need to make the motion regular, is one more integral of motion for any value of the first one (angular momentum). At first glance, it's not evident, that we can find the needed forces (among those physically feasible), especially when we deal with the fields of the counter beam. But they exist, and we present two interesting examples, which can be already useful for practice (main results below on integrable systems for accelerators were presented earlier in [15],[16]).

## 2.3 First integrable example of the round colliding beams

Let us take a drift space with the unity length (for simplicity) and a thin lens. The map for coordinates $x, y$ and angles $x', y'$ is:

$$\overline{x} \;=\; x + x'$$

$$\begin{aligned} \overline{y} &= y + y' \\ \overline{x}' &= x' + \frac{\overline{x}}{\overline{r}} \cdot U'(\overline{r}) \\ \overline{y}' &= y' + \frac{\overline{y}}{\overline{r}} \cdot U'(\overline{r}), \end{aligned} \tag{18}$$

where $U'(r) = -2r - \frac{cr}{ar^2+d}$, and $a, b, c$ are arbitrary constants, and $r = \sqrt{x^2+y^2}$. In other words we have linear transformation with $2 \times 2$ matrix of

$$\begin{pmatrix} 1 & 0 \\ -2 & 1 \end{pmatrix} \cdot \begin{pmatrix} 1 & 1 \\ 0 & 1 \end{pmatrix}$$

for both $x$ and $y$ phase spaces, followed with the radial kick of $-\frac{cr}{ar^2+d}$, which can be made remarkably close to the beam-beam kick from a short round bunch, because of the same "zero" and "infinity" asymptotic for the both cases.

One can check, that besides the angular momentum, there is another invariant for any value of the angular momentum $\mathcal{M} = xy' - yx'$:

$$I = (a \cdot r^2 + b)(p - r)^2 + c(p - r) + b(r^2 + \mathcal{M}^2/r^2). \tag{19}$$

In Fig.1(top) the particle's motion for this map is shown. Even near resonances this motion is regular. For comparison purposes, we present the motion for the same map with distorted linear transformation of $x, x'$ (Fig.1(bottom)) – $X$ matrix here is:

$$\begin{pmatrix} 1 & 0 \\ -1.9 & 1 \end{pmatrix} \cdot \begin{pmatrix} 1 & 1 \\ 0 & 1 \end{pmatrix},$$

which does not conserve the angular momentum. The corresponding motion looks like diffusion, and the $x$ and $y$ amplitudes significantly grow after a larger number of turns.

How to create this map practically? One just has to eliminate nonlinear perturbations over the ring, make the both tunes equal to 1/4 (these are the tunes of the necessary linear transformation), make short round beam (in comparison with $\beta$-function at the IP), and provide the distribution of counter beam close to one which produces the kick of $-\frac{cr}{ar^2+d}$ (it is the distribution of $\rho(r) \propto \frac{1}{(ar^2+d)^2}$).

A general approach for finding the integrable dynamical systems with additional integrals of motion is presented in Section 3.

## 2.4 Second integrable example of the round colliding beams.

Now we present a dynamical system with two invariants, which can be derived by means of usual accelerator theory tools. Let's take 1D equation of particle's motion in an accelerator:

$$x'' + g(s)x = F(x, s), \tag{20}$$

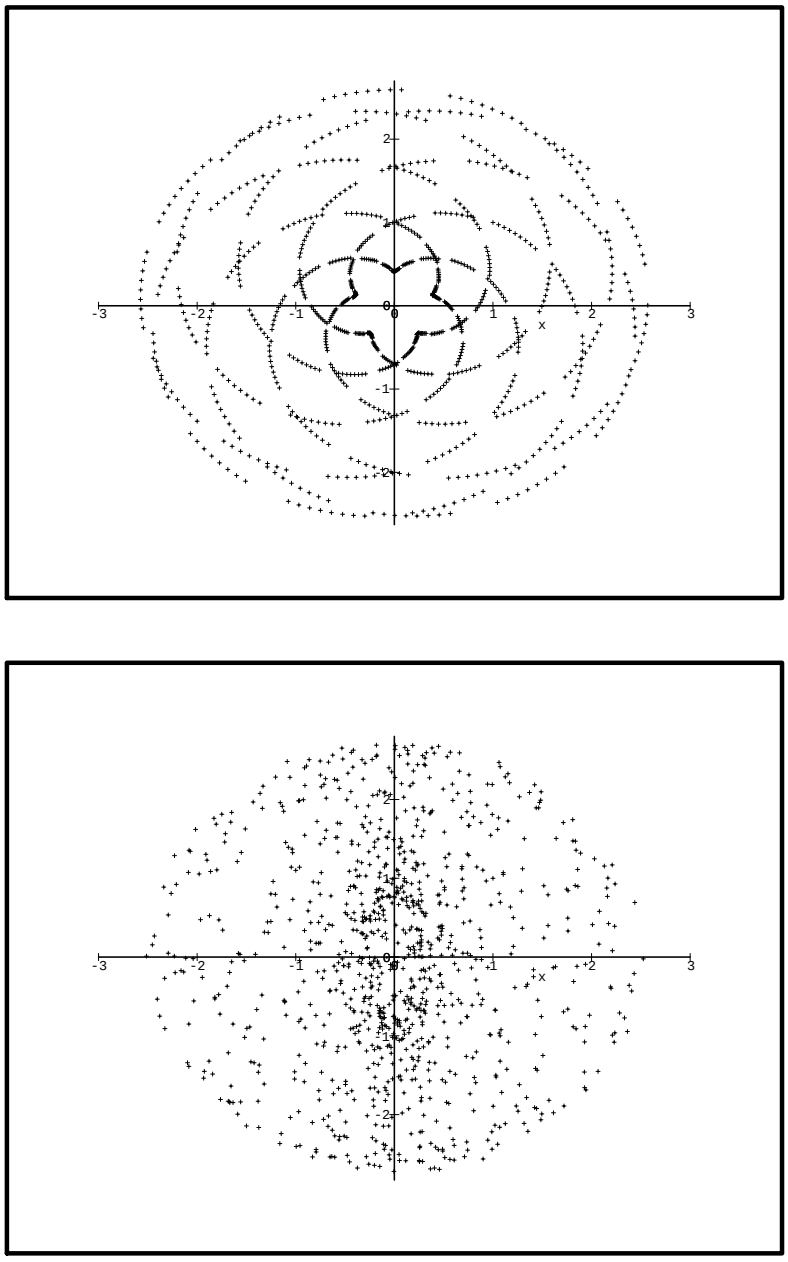


Figure 1: $X$-$Y$ plane of the integrable map of example 1 (top) and the map without conservation of the angular momentum (bottom). The parameters of the kick are: $c = -2, a = 1, d = 1$. The initial conditions are: $x = 0, x' = 1, y = 1, y' = 0$.

where $g(s)$ is the focusing function and $F(x,s)$ is an arbitrary force. This equation can be simplified by using the betatron phase $\psi = \int ds/\beta(s)$ instead of $s$ and changing the physical variable $x$ to the normalized variable $x_n = x/\sqrt{\beta(s)}$:

$$x_n'' + x_n = \beta^{3/2} F(x_n \cdot \sqrt{\beta}, s(\psi)). \tag{21}$$

The force due to round counter beam with the transverse Gaussian distribution can be presented as:

$$F_{rb} = -2\frac{N \cdot e^2}{\gamma m c^2} \frac{1 - \exp(-\frac{r^2}{2\beta\varepsilon})}{\frac{r}{\sqrt{\beta}}} \cdot \frac{f(\delta - 2s)}{\sqrt{\beta}}, \tag{22}$$

where $\varepsilon$ is the emittance of the opposite beam, $f$ is the longitudinal distribution of counter beam ( $\int f d\delta = 1$), $\delta$ is the longitudinal position of the test particle in the weak bunch with respect to the bunch center. The "time" $s = 0$ corresponds to the moment when the central test particle ($\delta = 0$) meets the center of the strong bunch.

The equation of particle motion in the interaction region in terms of $r = \sqrt{x^2 + y^2}$ is:

$$r'' + g(s)r = F_{rb} + \mathcal{M}^2/r^3, \tag{23}$$

where the last term means the "centrifugal" force.

Now let us consider a case when the weak bunch of the test particles is short with respect to the beta function at the IP and we can put $\delta = 0$, and at the same moment, the longitudinal charge distribution of the strong bunch (e.g. proton one in the Tevatron) is proportional to the inverse $\beta$-function:

$$f(2s) = C/\beta(s) = C/(\beta^* + s^2/\beta^*), \tag{24}$$

where $C$ is a constant, $\beta^*$ is the $\beta$-function value at the IP.

After substitution of the normalized variable $r_n = r/\sqrt{\beta(s)}$ and replacement of $s$ by the phase $\psi$, one gets:

$$r_n'' + r_n = \mathcal{M}^2/r_n^3 - C \cdot 2 \cdot \frac{Ne^2}{\gamma m c^2} \cdot \frac{1 - \exp(-r_n^2/2\varepsilon)}{r_n}. \tag{25}$$

One can see, that the force in this equation does not depend on time, and therefore, this 1-D equation is integrable. The coordinate dependence on time can be found with use of common 1-D formulas.

The trick with obtaining the time-independent force is related with the fact, that the 'centrifugal' force is invariant under substitution of new variables and changing 'time' to the betatron phase. Fig. 2 presents the potential of this motion which looks like the potential of a gravitational center. It's easy to prove, that the force in (25) has one zero for a counter beam with opposite sign of electric charge.[3]

[3] After multiplying the force by $r_n^3$ and after putting it equal to zero, we have:

$$r_n^4 + C \cdot 2 \cdot \frac{Ne^2}{\gamma m c^2} \cdot (1 - \exp(-r_n^2/2\epsilon)) \cdot r_n^2 = \mathcal{M}^2.$$

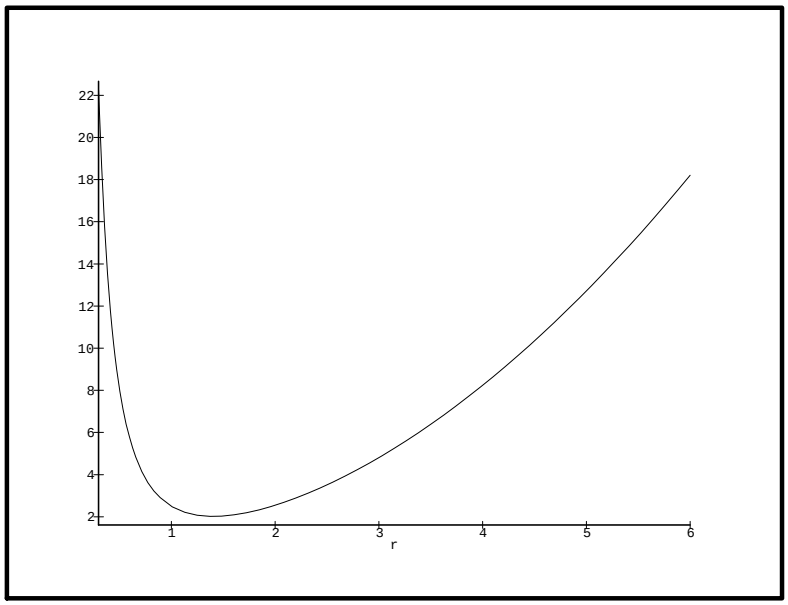


Figure 2: The potential for equation (25) with $\mathcal{M} = 2$ and with the tune shift from the counter beam of $\xi = \frac{Ne^2}{4\pi\gamma mc^2\varepsilon} = .05$.

If one wants to realize this strategy in practice, then one has to create the longitudinal distribution in the form of Eq.(24) over some wide range of $s$, and to make it zero at $s$. Next step is to make a linear transformation to the next interaction region without any phase advance [4] (we only have to reverse the sign of $\beta$-function derivative), and then, if we have the same counter beam with the same distribution (and so on periodically), we have a system with the needed equation of motion. Of course, it's difficult to create such a longitudinal distribution on the tails of strong bunch, but it's obvious, that if we have some difference between the distribution and the inverse $\beta$-function for $s \gg \beta^*$, we probably can neglect the perturbation. One can see, that the Gaussian betatron distribution does not play a role here: it can be replaced with any smooth function of $r$, the only condition one needs is the possibility to present $r_n$-$s$ distribution in the factorized form.

What is more essential, that the working point of this system is near the half-integer resonance, when the number of interaction points is odd, and near the integer resonance, when this number is even. So, perturbations of the arcs of collider de-

The left hand side (L.H.S.) of this equation is a monotonical rising function so it has the only intersection with a constant in the R.H.S. So we have only one zero for this force (in the graph of potential it corresponds to its minimum). So the presented system has no fixed points besides the only stable one, hence no resonances and separatrices.

[4] Actually, we can change both $x - y$ phases on $\pi$. We obtain the same motion for $r, r'$ due to symmetry of potential of this motion. In this case we always stay near the integer resonance.

termine the permissible distance of the working point from the resonance, and, consequently, determine the accuracy of the conservation of integrals (this situation is common for integrable systems: perturbations almost always lead to a small stochasticity in nearly integrable systems, the issue is in allowable values of perturbations).

One more remark is needed. The weak bunch (e.g., antiprotons in the Tevatron) has a small longitudinal size in our dynamical system (while the longitudinal distribution of the strong bunch is taken proportional to the inverse $\beta$-function). If its length is not small in comparison with the $\beta$-function, than the force becomes to be time-dependent for particles with energy off-sets and large respective deviations $\delta$ even in the normalized variables. We have made a check whether it is important or not by simulation (see Section 4).

In the following Section a formal construction of the integrable systems applicable to accelerators will result in derivation of the above examples in a regular way.

# 3 1D Dynamical Systems with Invariants, Polynomial in Momentum

In this section we construct, at first, model accelerator lattices with one cell consisting of a drift space and a thin nonlinear lens. In the map considered, we put $p = x'$, where $x'$ is the particle trajectory slope, and take the drift length $l = 1$ to simplify formulas. The map corresponding to one cell is:

$$\begin{aligned} \overline{x} &= x + p\,, \\ \overline{p} &= p + f(\overline{x})\,. \end{aligned} \tag{26}$$

Here $x$, $p$ are the initial values and $\overline{x}$, $\overline{p}$ are the final values of the coordinate and momentum, $f(\overline{x})$ is the kick function of the nonlinear lens to be found jointly with the desired invariant.

Let's search it in the form of a polynomial, quadratic in momentum. The equation for an invariant $I$ is:

$$A(\overline{x})\overline{p}^2 + B(\overline{x})\overline{p} + C(\overline{x}) \equiv A(x)p^2 + B(x)p + C(x)\,. \tag{27}$$

where $A(x), B(x), C(x)$ are any analytic functions of the coordinate. The kick $f(x)$ of the nonlinear lens is also assumed to be an arbitrary analytic function of $x$.

The equation should be valid for all $x$ and $p$. In particular, at $p = 0$, (or $x = \overline{x}$) we can find the kick function from previous expression: $f(x) = -B(x)/A(x)$, as expressed through the other unknown functions. Substituting $f(x)$ back into (27) we can obtain a general form of $A(x), B(x), C(x)$ by comparison of the L.H.S. and R.H.S. (one can find the details in [16, 15]). The general form of invariant is:

$$\begin{aligned} \mathcal{I}(x,p) = (a_2x^2+a_1x+a_0)p^2 + (2a_2x^3+3a_1x^2 \\ +b_1x+b_0)p + a_2x^4+2a_1x^3+b_1x^2+2b_0x \end{aligned} \tag{28}$$

and the kick function $f$ is given by:

$$f(x) = -\frac{2a_2x^3 + 3a_1x^2 + b_1x + b_0}{a_2x^2 + a_1x + a_0}\,. \tag{29}$$

Similar map was presented earlier in [17].

## 3.1 Invariants polynomial in momentum

The previous example dealt with the systems where the time dependence was represented by delta-functional non-linear kick functions, and the invariants were quadratic in momentum only at the kick moment. Here we construct a family of continuous time-dependent 1-D Hamiltonians which have a quadratic invariant, and thus the respective motion in 1.5-D is integrable. Consider a general form of invariant quadratic in momentum $p$, assuming that the coefficients $A$, $B$, $V$ are arbitrary functions of time $t$ and coordinate $x$:

$$I = \frac{1}{2}(Ap - B)^2 + V\,,$$

$A \neq 0$. Equating its total time derivative to zero, we account for the Hamiltonian equations of motion $\dot{x} = p\,,\ \dot{p} = f$, where the unknown force $f$ depends on $t$, $x$

$$\frac{dI}{dt} = (Ap - B)\Big(A_xp^2 + (A_t - B_x)p + Af - B_t\Big) + V_xp + V_t \equiv 0\,,$$

the subscripts here denote the respective partial derivatives. The vanishing coefficients of each power of $p$ yield a set of equations in partial derivatives for the four unknown functions: $f$ is to be found along with $A$, $B$, $V$.

First of all, $A_x = 0$, and $A = A(t)$ is an arbitrary function of time. Then we take $A_t - B_x = 0$, whence:

$$B(x,t) = \dot{A}x + A^2\dot{D}\,,$$

with an arbitrary $D(t)$; dots denote the time derivatives. We choose here the special form of arbitrary additive function of time for future convenience.

The last two equations form a set of equations specifying the unknowns $f$ and $V$:

$$A(Af - B_t) + V_x = 0 \tag{30}$$

$$-B(Af - B_t) + V_t = 0 \tag{31}$$

The force $f$ is thus expressed via $V$, $B$, $A$:

$$f = -\frac{V_x}{A^2} + \frac{B_t}{A}\,, \tag{32}$$

and $V$ is determined by the homogeneous equation in partial derivatives of the 1st order:

$$B\,V_x + A\,V_t = 0$$

Its characteristic curve $x(t)$ is then obtained from the equation:

$$\frac{dx}{dt} = \frac{B}{A} = \frac{\dot{A}x + A^2\dot{D}}{A}\,.$$

Integration gives the lines of constant level of $V$:

$$X \equiv \frac{x}{A(t)} - D(t) = const\,.$$

Hence,

$$V(x,t) = U\Big(\frac{x}{A(t)} - D(t)\Big)\,,$$

where $U(X)$ is an arbitrary function.

Thus we conclude, that the general solution to our problem of integrable system in 1.5D with quadratic invariant is generated with three arbitrary functions: $A(t)$, $D(t)$, $U(X)$. The corresponding force $f$ is then found from (32):

$$f = -\frac{1}{A^3}U' + \frac{1}{A}(\ddot{A}x + (A^2\dot{D})^{\cdot})\,.$$

The Hamiltonian of this system can be found from the expression for $f$:

$$\mathcal{H}(x,p,t) = \frac{p^2}{2} + \frac{1}{A^2}U(\frac{x}{A} - D) - \frac{A\ddot{A}}{2}(\frac{x}{A})^2 - (A^2\dot{D})^{\cdot}\frac{x}{A}\,,$$

and the final form of the desired invariant is:

$$I = \frac{1}{2}(Ap - \dot{A}x - A^2\dot{D})^2 + U(\frac{x}{A} - D)\,.$$

Let's look at this result from another point of view. Starting from a Hamiltonian which is independent of the time variable $T$ (with the particle mass $m = 1$):

$$H(X,P) = \frac{P^2}{2} + U(X)\,, \tag{33}$$

we can apply a time-dependent (canonical) transformation of the dynamic variables along with a relevant transformation of the time variable $T(t)$:
$X(T), P(T) \stackrel{T(t)}{\longrightarrow} x(t), p(t)$, so that the Hamiltonian will take the form:

$$\mathcal{H}(x,p,t) = \frac{p^2}{2} + \mathcal{U}(x,t)\,. \tag{34}$$

**Transformation** 1° is additive, use is made of any coordinate displacement function of time $D(t)$:

$$\begin{aligned} t &= T, \\ x &= X + D(t), \\ p &= P + \dot{D}(t)\,, \end{aligned} \tag{35}$$

here 'dot' stands for the time derivative. The time-dependent Hamiltonian of the new system has the form (34):

$$\mathcal{H} = \frac{p^2}{2} + U(x - D(t)) - x \cdot \ddot{D}(t)\,. \tag{36}$$

Apparently, the invariant of this 1.5D system is given by the function $H(X,P)$ of Eq. (33) where $X, P$ should be expressed in terms of the new variables $x, p$:

$$H = \frac{1}{2}(p - \dot{D}(t))^2 + U(x - D(t)) = const\,. \tag{37}$$

**Transformation** 2° applies an arbitrary time-dependent coordinate normalization function $A(t)$ and involves a corresponding transformation of the time variable $T \to t$:

$$\begin{aligned} dt &= A^2 dT, \\ x &= AX\,, \\ p &= A\dot{X} + \dot{A}X = \frac{P}{A} + \dot{A}X, \end{aligned} \tag{38}$$

where 'dot' denotes differentiation with respect to the new time $t$ and use is made of the Hamiltonian equation $dX/dT = P$ in the last line. By its definition, $p = \dot{x}$, while the second Hamiltonian equation:

$$\dot{p} = \frac{\dot{P}}{A} - P\frac{\dot{A}}{A^2} + \dot{A}\dot{X} + \ddot{A}X = -\frac{U'}{A^3} + \ddot{A}X$$

yields the desired time-dependent Hamiltonian function:

$$\mathcal{H} = \frac{p^2}{2} + \frac{1}{A^2}U(\frac{x}{A}) - \frac{\ddot{A}}{A} \cdot \frac{x^2}{2}\,. \tag{39}$$

Again the invariant of this 1.5D integrable system is available from (33): using (39) we express $X, P$ via $x, p$ and obtain:

$$H = \frac{1}{2}(Ap - \dot{A}x)^2 + U(\frac{x}{A}) = const\,. \tag{40}$$

This expression is a generalization of the Courant-Snyder invariant of the linear systems[5]. One can check directly, that Example 2 in the previous section results from 2°.

[5] Indeed, Hill's equation $\ddot{x} + g(t)x = 0$ implies $\mathcal{U} = g(t)x^2/2$ in (34). Taking $U(X) = X^2/2$ in (33) we immediately obtain from (39): $\ddot{A} + g(t)A = A^{-3}$, *i.e.* the well-known equation for the betatron amplitude function, hence $A(t) = \sqrt{\beta}$, and (40) takes the usual form of the Courant-Snyder invariant. We see that $x, p$ correspond to the conventional betatron variables, $t$ is the machine azimuth, while $X, P$ are the normalized betatron variables and $T$ stands for the betatron phase advance.

Any combination of transformations 1° and 2° also provides an integrable system of the form (34). Note that any integrable system produced with this technique involves three arbitrary functions: $U(X), D(t)$ and $A(t)$. So the combination of 1° and 2° produces all the dynamical systems with invariants quadratic in momentum.

Having in mind 1° and 2°, we can at once express an invariant cubic in $p$ in the efficient general form:

$$\mathcal{I}(x,p,t) = \frac{1}{3}(Ap-B)^3 + U(X,T)(Ap-B) + V(X,T) \tag{41}$$

with $B = \dot{A}x + A^2\dot{D}$, $A \neq 0$ and $D$ being arbitrary functions of time *only*, and the new variables $X(x,t) = x/A - D$ and $T(t) = \int dt/A^2$. The invariance condition relates $U$ and $V$ by a set of quasilinear equations in partial derivatives (the latter are denoted with corresponding subscripts):

$$\begin{aligned} V_X + U_T &= 0\,, \\ V_T - UU_X &= 0\,, \end{aligned} \tag{42}$$

and gives the expression for the force $f$:

$$f(x,t) = -\frac{1}{A^3}U_X + \frac{1}{A}(\ddot{A}x + (A^2\dot{D})^{\cdot})\,. \tag{43}$$

Equations (42) are similar to those of transonic flow in fluid dynamics, in inverse functions they convert into *linear* Tricomi's equation. Provided $U < 0$ everywhere, we come to the hyperbolic type in $U_{TT} + (UU_X)_X = 0$, thus the (periodic) Cauchy problem will bring in two free functions of $t$ on the axis $x = 0$. These together with $A, D$ give us a sufficient freedom to specify at $x = 0$ any periodic $f, f_x$ and $f_{xx}$, i.e. the assigned gradient and sextupole component functions in the lattice together with $f = 0$ on the closed orbit.

So, the main result of the previous calculations is in fact, that dynamical systems with invariants up to the third order in momentum can be obtained by linear tools! May be it is valid for quartic in momentum invariants (what we need is to find some substitution for unknown functions to get a linear equation for them; for cubic invariants this is Tricomi's equation, for example); the first example with thin lens was obtained by linear calculation and apart from the lens position this invariant is quartic in momentum.

## 3.2 How to select integrable dynamical systems for round beams from the variety of 1D integrable systems

So now we know, how to construct 1D integrable systems. What is the difference between a common 1D case and 2D systems with conservation of the angular momentum? Actually a 2D system with the angular momentum conservation can be

reduced to a 1D system with the 'centrifugal' force $\mathcal{M}^2/x^3$. But the difference is in the condition, that the second invariant for this system must exist for each value of $\mathcal{M}$. For $\mathcal{M} = 0$ we have a usual 1D system, so the desired integrable system for round beams is a common 1D integrable system, but in general the converse statement is not true. So the family of integrable systems for round beams is less than or equal to the family of common 1D integrable systems.

Let's take an example with thin lens and drift space and write the map for $r = \sqrt{x^2 + y^2}, r'$:

$$r_n = \sqrt{r^2 + 2rr' + r'^2 + \mathcal{M}^2/r^2},$$

$$r'_n = \frac{rr' + r'^2 + \mathcal{M}^2/r^2}{\sqrt{r^2 + 2rr' + r'^2 + \mathcal{M}^2/r^2}} + k(r_n),$$

where $k(r_n)$ is the nonlinear kick. After taking the invariant in the form, quadratic in momentum, we obtain, as earlier, equations for $k(r_n), A, B, C$, and we have to find such functions that form the invariant for an arbitrary value of $\mathcal{M}$. One can check, that this invariant is

$$I = (a \cdot r^2 + b)(p - r)^2 + c(p - r) + b(r^2 + \mathcal{M}^2/r^2),$$

and the kick is

$$k(r) = -2r - \frac{cr}{ar^2 + d}.$$

The first example for round beams in the previous section is what we have derived here as a one lens system with invariant, quadratic in momentum. One can check, that the invariant is conserved for each $\mathcal{M}$. In comparison with the same simple 1D system, we have two free parameter less here; it corresponds to the statement in the beginning of this subsection.

Let's now take a quadratic in momentum invariant with a continuous time dependence:

$$I = \frac{1}{2}(Ap - \dot{A}x)^2 + U(\frac{x}{A}) \, .$$

The corresponding force $f$ is:

$$f = -\frac{1}{A^3}U'(\frac{x}{A}) + \frac{1}{A}\ddot{A}x \, .$$

Let's take some force from this set, assuming that the angular momentum is equal to zero. Then let's add the 'centrifugal' term $\mathcal{M}^2/x^3$ to our force. One can check, that it is just changing $U'$ to $U' - \mathcal{M}^2/x^3$, so the new force belongs to our set too. It means, that these dynamical systems give totally integrable systems for round beams (see example 2 for round beams in the previous section).

Let's look now at systems with invariants quartic in momentum. There exist very interesting examples of integrable dynamical systems for round beams. Besides, it's useful to see an application of techniques for finding invariants for round beams.

### 3.3 Integrable systems with soliton-like forces

Let's take the simplest quartic polynomial as an invariant:

$$I = p^4 + A(x,t)\cdot p^2 + B(x,t)\cdot p + C(x,t);$$

here we omit the cubic terms at all, $A, B, C$ are unknown functions. After differentiation of this invariant w.r.t. to time we should have zero coefficients of each power of $p$ (since $dI/dt = 0$), so we have the following set of equations:

$$\begin{aligned} 4F + \frac{\partial A}{\partial x} &= 0 \\ \frac{\partial A}{\partial t} + \frac{\partial B}{\partial x} &= 0 \\ 2\cdot A\cdot F + \frac{\partial B}{\partial t} + \frac{\partial C}{\partial x} &= 0 \\ BF + \frac{\partial C}{\partial t} &= 0, \end{aligned} \tag{44}$$

where $F = \dot{p}$ is the force.

Let's suppose, that we have found some solution of these equations. Now we want, that $F + \mathcal{M}^2/x^3$ be also a solution of the previous set of equations. From the first line of (44) we see, that $A$ has to be transformed into $A + 2\mathcal{M}^2/x^2$, and $B$ stays unchanged.[6]

Let's eliminate the function $C$ from the equations. We can just take the partial derivative of the third equation in (44) w.r.t. to $t$, and the partial derivative of the forth one w.r.t. to $x$, and subtract one from another. We have:

$$2\frac{\partial(A\cdot F)}{\partial t} + \frac{\partial^2 B}{\partial t} = \frac{\partial(B\cdot F)}{\partial x}.$$

Let's put here the new $A$ and $F$. We have:

$$2(A_t\cdot F + A\cdot F_t) + 4\mathcal{M}^2/x^2\cdot F_t + 2\mathcal{M}^2/x^3\cdot A_t + B_{tt} =$$

$$B_x(F + \mathcal{M}^2/x^3) + B(F_x - 3\mathcal{M}^2/x^4);$$

here $A, B, F$ are the old functions independent of $\mathcal{M}$, subscripts $t, x$ mean partial derivatives w.r.t. to $t, x$.

We want to get solutions for an arbitrary value of the angular momentum, so we demand, that each coefficient at any power of $\mathcal{M}$ should vanish. So, from the previous equation we obtain two ones (without $\mathcal{M}$); adding to them the first two equations of

[6] This is not the only way of transformation of $A$ and $B$. For example, $A$ may get a term, which depends on time and momentum. But here we are looking for the simplest solutions.

(44) we have:

$$\begin{aligned} 4F + \frac{\partial A}{\partial x} &= 0 \\ \frac{\partial A}{\partial t} + \frac{\partial B}{\partial x} &= 0 \\ 3A_t \cdot F + 2A \cdot F_t + B_{tt} &= B \cdot F_x \\ 4F_t \cdot x^2 + 2A_t \cdot x &= B_x \cdot x - 3B. \end{aligned} \tag{45}$$

This is a set of four equations for three unknown functions. A check for consistency is needed in general, in order to verify the existence of any solutions.

To eliminate now $F$ and $B$, we take $F$ from the first and $B_x$ from the second equation and substitute these in the last one (having taken its time derivative). After that we get an equation for $A$:

$$x^2 A_{xxt} - x A_{xt} = 0.$$

All the solutions are:

$$A = f_1(t)x^2 + f_2(t) + g(x);$$

here $f_1, f_2, g$ are free functions.

After that we have to use one more equation for $A, B, F$, namely the third one in the set (45). At first, let's express $F$ and $B$ using the solution for $A$. From the first equation of (45) we have:

$$4F = -2f_1(t) \cdot x - g'(x),$$

and from the second and last ones we have:

$$3B = -3(f_1'(t) \cdot x^3 + f_2'(t) \cdot x) + 2f_1'(t) \cdot x^3.$$

Let's put $f_2 = 0$ for saving calculations (the case $f_2 \neq 0$ can be treated in the same way, but with more complications). Then $b = -f_1' x^3/3$.

The third equation of (45) now reads:

$$3f_1'(t) \cdot x^2 \cdot (\frac{-2f_1(t) \cdot x - g'(x)}{4}) - (f_1(t) \cdot x^2 + g(x))f_1'(x) \cdot x - f'''(t) \cdot x^3/3 =$$

$$f_1'(t) \cdot x^3/3 \cdot (\frac{2f_1(t) + g''(x)}{4}).$$

We rewrite it in a more compact form:

$$(-8/3 \cdot f_1(t)f_1'(t) - f_1'''(t)/3) \cdot x^3 = f_1'(t)(3g'(x)x^2/4 + g''(x) \cdot x^3/12 + g(x) \cdot x).$$

Having thus separated the variables, we now have:
1. $f_1(t) = const$, $g$ is an arbitrary function of $x$. It's the case of the invariant quadratic

in momentum; now we have it squared.
2.

$$3g'(x)x^2/4 + g''(x)\cdot x^3/12 + g(x)\cdot x = -h\cdot x^3, \tag{46}$$

where $h$ is an arbitrary constant. For $f_1(t)$ we have:

$$f_1''' + 8\cdot f_1\cdot f_1' - 3\cdot h\cdot f_1 = 0. \tag{47}$$

This reminds the equation for a traveling wave solution $f(x-ct)$ of the Korteweg–de Vries equation:

$$f''' + f\cdot f' - c\cdot f' = 0.$$

After changing $f_1$ to $f/8$ and $3h$ to $c$ in (47), we come to this equation. Then we can find $g$ from (46). Our force then is equal to

$$F(x,t) = -f_1(t)\cdot x/2 - g'(x)/4.$$

So, the presented above method gives an analytical tool aimed at finding integrable systems for round beams (or, even for systems with more complicated integrals of motion, than the angular momentum). May be it is possible to use numerical methods, presented in [18], to this end. One more way is to apply Lie groups and the inverse scattering transform to this problem; this approach is now under development.

# 4 Beam-beam Simulations with Round Beams in Tevatron

## 4.1 Beam-beam simulation code and parameters of the Tevatron upgrade

The Tevatron collider upgrade (TeV33) [19] intends to operate with some hundred bunches in each beam. Large number of bunches $N_b$ results in small bunch spacing of 132 ns (or about 40 m) and, therefore, collisions occur more frequently. Such a manner to increase the luminosity of the machine where colliding beams share the same vacuum chamber yields in $2(N_b-1)$ parasitic collisions besides specially designed interaction points (IPs). Detrimental effects of the parasitics collisions of high current beams can be reduced by separation of the orbits of $p$ and $\bar{p}$ beams everywhere except the IPs. However, due to limited space available and limited strength of electrostatic separators several crossing points around the IPs can not be effectively treated in such a way. Collision with crossing angle allows to increase the separation up to a safe value. For design parameters of the TeV33, the half-angle of about $\phi$ =0.15–0.2 mrad leads to some 2.5–3 rms beam size separation at the first parasitic crossing [20]. Our studies do not cover the issues of the long range collisions at the parasitic crossings, but we do investigate the effects of the crossing angle at the IPs.

We employ a recently developed beam-beam simulation code BBC Ver.3.3 [21] developed by K.Hirata [21] for the beam-beam simulations in "weak-strong regime" which is close to the TeV33 conditions where proton bunch population is about 6 times the antiproton one. The "weak" (antiproton) bunch was presented by number of test particles, while the "strong" (proton) bunch appeared as an external force of Gaussian bunch. Essential features of the code are:
a) fully symplectic synchrobetatron mapping;
b) Lorenz transformation of the collision with the angle to a head-on collision;
c) inclusion of the bunch-length effects by using several slices in strong bunch;
d) variation of the beta function $\beta$ along the bunch during collision;
e) energy loss due to longitudinal electric fields are included too.

Typically we tracked 100 (maximum 1000) test particles through five slices of strong bunch for (50-100)$\cdot 10^3$ turns. Typical number of 50,000 turns corresponds to about 1 s in TeV'33, it is some 200 synchrotron oscillation periods. No damping due to radiation or cooling is assumed to play role in the beam dynamics. Further increase of the number of particles as well as number of slices gave almost identical results. Version 3.3 of the BBC code (Dec.1995) assumes the crossing angle only in one plane (e.g. horizontal).

The code outputs of greatest practical utility are luminosity, rms beam sizes and maximum betatron amplitudes which any of the test particles attained during tracking. These outputs are given with respect to unperturbed values, e.g. sizes and amplitudes are divided by their design rms values $\sigma_{x,y}/\sigma^0_{x,y}$ and $A^{max}_{x,y}/\sigma^0_{x,y}$, the luminosity is presented by the reduction factor of $R = L/L_0$ where the bare design luminosity $L_0 = f_0 N_p N_{\bar{p}}/(4\pi\sigma^0_x\sigma^0_y)$ and $f_0$ is the rate of collisions.

The relevant parameters of the simulations were chosen close to the TeV'33 design ones [19] and presented in the Table 1.

## 4.2 Three round beams schemes

Three schemes of Tevatron with round beams were used for simulations. The first one is usual linear structure with equal horizontal and vertical emittances and equal beta-functions at Interaction Point (IP). That is represented in the BBC code as the following transformation:

$$Beam-Beam\,Collision\,(BBC) \rightarrow Arc \rightarrow BBC \rightarrow Arc \rightarrow etc.$$

Note, that the BBC part operates with physical variables $x, x', y, y'$ while the transformation in the arc operates with the normalized variables $x/\sqrt{\beta_x}, x'\sqrt{\beta_x}, y/\sqrt{\beta_y}, y'\sqrt{\beta_y}$.

The second option is so called "Mobius" ring proposed by R.Talman [10] in which one 90° rotation of betatron plane takes place every turn. If we mark the rotation as $R(\pi/2)$ then in simulations the Mobius scheme looks like

$$BBC \rightarrow Arc \rightarrow R(\pi/2) \rightarrow etc.$$

Table 1: Parameters of TeV33 and those used in simulations.

| | | TeV33 | Simulations | |
|---|---|---|---|---|
| Energy | $E$ | 1000 | 1000 | GeV |
| $p, \bar{p}$/bunch | $(N_p, N_{\bar{p}})$ | (30, 6) $\cdot 10^{10}$ | (see $\xi$) | |
| Number of IPs | $N_{IP}$ | 2 | 1 | |
| Energy spread, rms | $\sigma_E = \Delta E/E$ | $\sim 2 \cdot 10^{-4}$ | $2.2 \cdot 10^{-4}$ | |
| Bunch length, rms | $\sigma_z$ | 18 | 15 | cm |
| Synchrotron tune | $\nu_z$ | $\sim$0.0045 | 0.0045 | |
| Emittance, rms | $\varepsilon_{x,y}$ | $\sim 3 \cdot 10^{-9}$ | $3 \cdot 10^{-9}$ | m·rad |
| Beta-function at IP | $\beta^*_{x,y}$ | 35 | 25 | cm |
| $\bar{p}$ Beam-beam parameter | $\xi$ | 0.022 (two IPs) | 0.05 (0$\rightarrow$0.5) | |
| Crossing half-angle (design) | $\phi$ | $\simeq 0.15$ | 0; 0.1; 0.2 | mrad |

A special insertion is placed in the point with equal horizontal beta functions and their derivatives, so we can easily calculate new tunes of the ring versus the old ones. For normalized variables the one-turn matrix is

$$M = \begin{pmatrix} 0 & I \\ -I & 0 \end{pmatrix} \cdot \begin{pmatrix} T_x & 0 \\ 0 & T_y \end{pmatrix} = \begin{pmatrix} 0 & T_y \\ -T_x & 0 \end{pmatrix}, \tag{48}$$

where $I$ is the identity $2 \times 2$ matrix and the bare arc transformation matrices are

$$T_{x,y} = \begin{pmatrix} \cos \mu_{x,y} & \sin \mu_{x,y} \\ -\sin \mu_{x,y} & \cos \mu_{x,y} \end{pmatrix}. \tag{49}$$

The eigenvalues of the matrix $M$ are:

$$\lambda_{\pm} = e^{i(\frac{\mu_x + \mu_y}{2}) \pm i\pi/2}, \tag{50}$$

and their complex conjugated ones. Therefore, the new tunes are:

$$\nu_{\pm} = \frac{\nu_x + \nu_y}{2} \pm \frac{1}{4}. \tag{51}$$

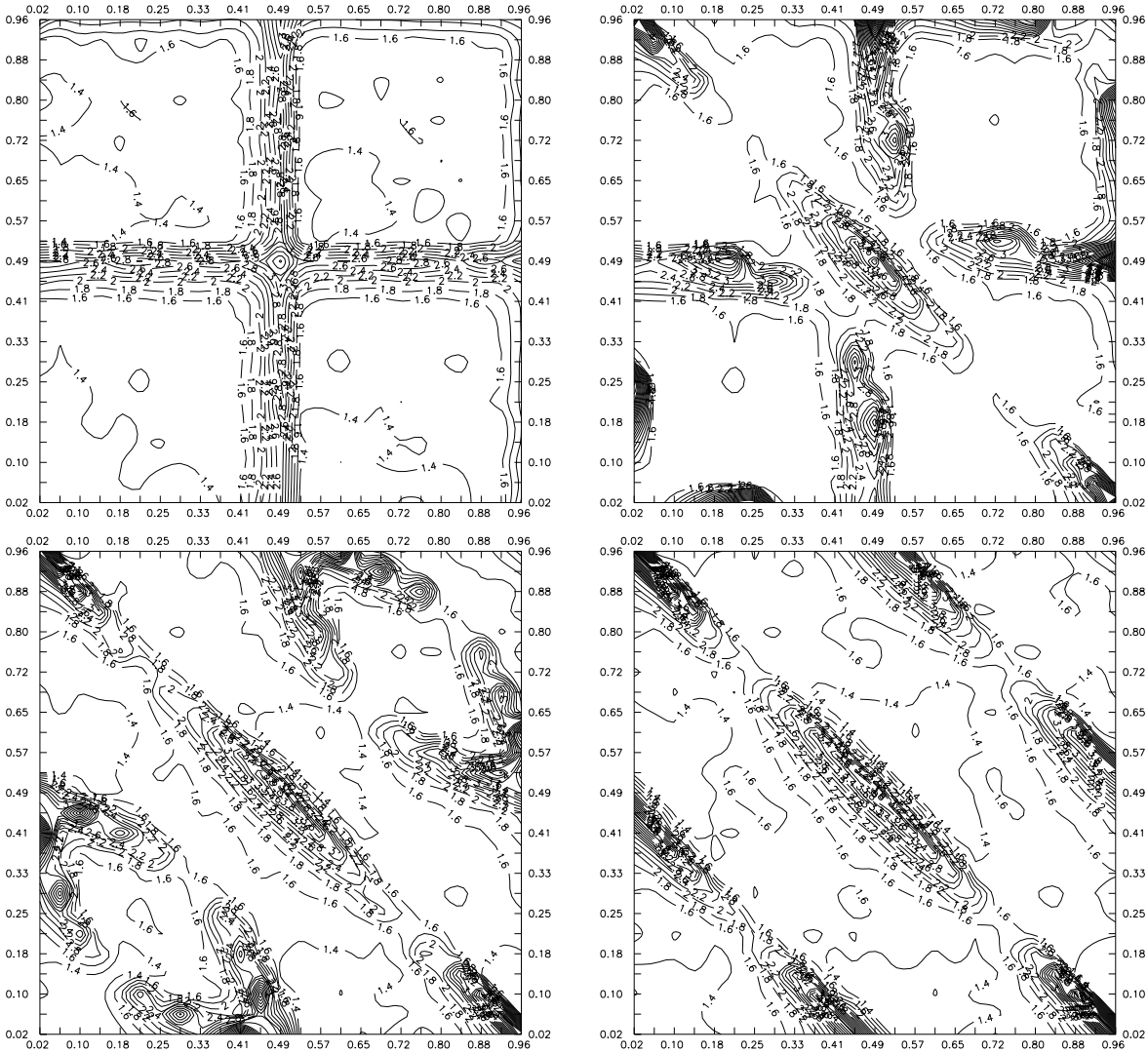

Figure 3: Contour plots of the rms beam size $\sqrt{(\sigma_x^2+\sigma_y^2)/\sigma_0^2}$ after 1000 turns vs betatron tunes of the lattice $\nu_x$ (horizontal axis) and $\nu_y$ (vertical axis), $\xi = 0.05$. **a** – top left – $R(0)$ no coupling in the lattice; **b** – top right – $R(\pi/6)$ coupling; **c** – bottom left – $R(\pi/3)$ coupling; **d** – bottom right – $R(\pi/2)$ Mobius coupling.

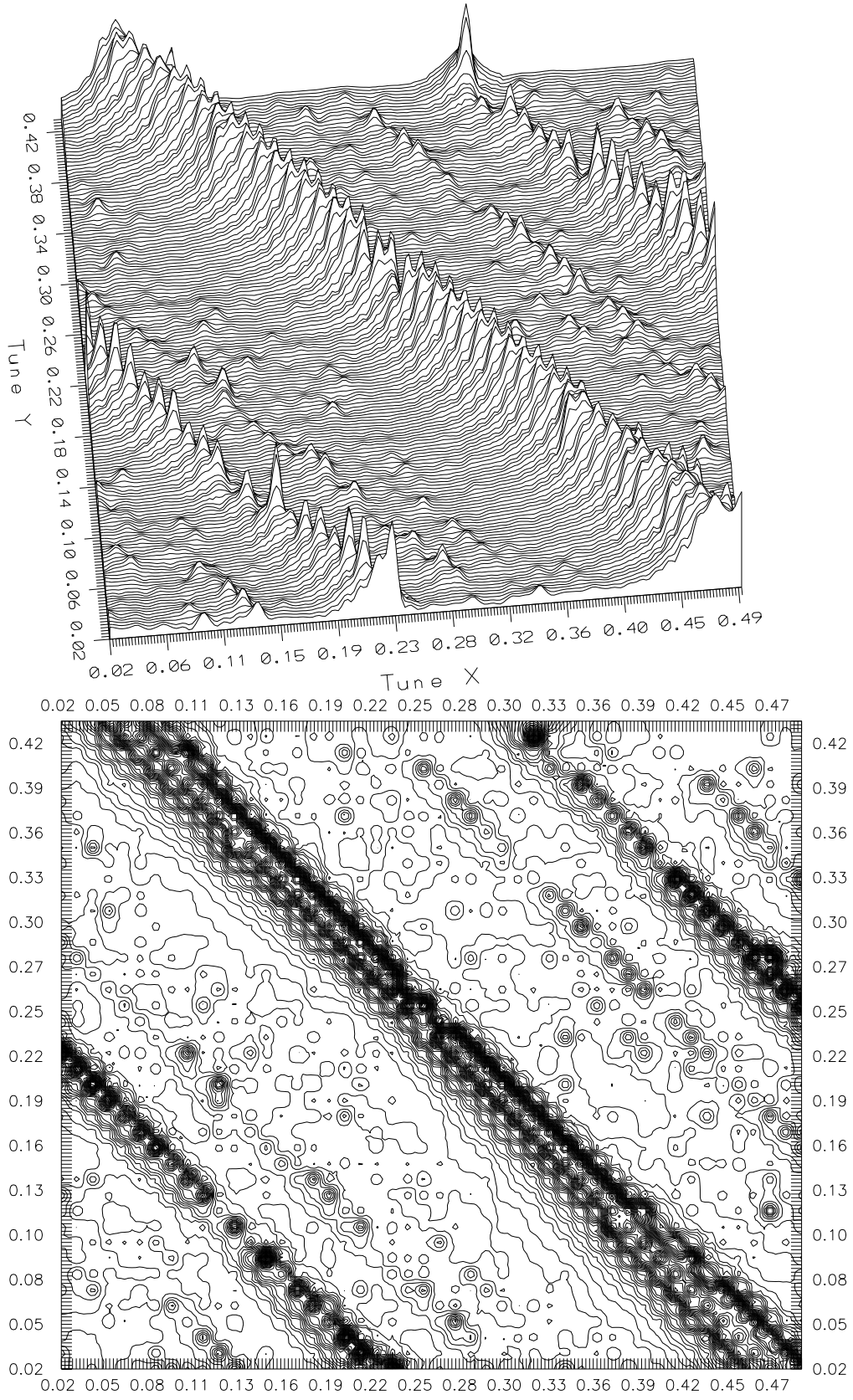


Figure 4: 3-D (upper) and contour (lower) plots of the maximum betatron amplitude $A_{max}/\sigma_0$ after 1000 turns vs betatron tunes of the lattice $\nu_x$ (horizontal axis) and $\nu_y$ (vertical axis), the Möbius scheme with $\xi = 0.05$.

The third variant is what the Novosibirsk $\phi$-factory suppose to exploit [4] – it has two "back-and-forth" rotation of the betatron oscillations plane on 90° angle without changing betatron tunes, or schematically:

$$BBC \rightarrow Arc \rightarrow R(+\pi/2) \rightarrow BBC \rightarrow Arc \rightarrow R(-\pi/2) \rightarrow etc.$$

These three schemes we denote below as $R(0)$, $R(\pi/2)$ or $M$ - for Mobius one, and $R(\pm)$, respectively. It's evident, that all the beam-beam interaction in the three cases have to give the same results for round beams, when there are no perturbations in the arcs.

It is interesting to trace how the resonances changes when strong $X-Y$ coupling is introduced. Fig.3a demonstrates the contour plot of the rms beam size factor $R_\sigma = \sqrt{(\sigma_x^2+\sigma_y^2)/\sigma_0^2}$ for round beams after 1000 turns vs. the arc tunes of $(\nu_x, \nu_y)$. The parameter of the beam-beam interaction is $\xi = 0.05$. One can see that major resonances of $\nu_x$ =0,0.5,1 and $\nu_y$ =0,0.5,1 manifest themselves as significant increase of $R_\sigma$ above its initial value of $\sqrt{2} \simeq 1.41...$ Introduction of the coupling matrix of $R(\pi/6)$ into one-turn transformation map – see Fig.3b leads to appearance of the diagonal central island along $\nu_y + \nu_x = 1$ line and its extension at $(\nu_x, \nu_y)$=(0,1), (1,0). Note, that area where the rms size is about 1.4 has shrunk significantly. In the next Fig.3c the coupling angle is increased to $\phi = \pi/3$ and, besides the diagonal line, four $V-$shape resonances lines are seen and some area with small size increase is seen again. Finally, with the Mobius coupling of $R(\pi/2)$ one can observe conjunction of those latter into resonances along $\nu_y+\nu_x = 0.5$ and $\nu_y+\nu_x = 1.5$ – see Fig.3d. Now the area where $R_\sigma \leq 1.4$ is rather wide. Thus, introduction of the Mobius coupling leads to one dimensional resonance set instead of two dimensional without the coupling.

The 1-D resonances along the lines of $\nu_y + \nu_x = rational$ are clearly seen in the contour plot of maximum betatron amplitude (1000 turns, 50 particles) $R_A = \sqrt{(A_{x,max}^2 + A_{y,max}^2)/\sigma_0^2}$ which is presented in Fig.4. To emphasize the high-order resonances we imply random betatron phase modulation (see below).

## 4.3 Comparison of RBs and non-RBs. Random tune modulation.

Fig.5 shows the maximum betatron amplitude after 100,000 "head-on" collisions of the round beams (Mobius scheme) without any other beam disturbances. One can see numerous resonances, the most strongest among them are at $\nu$ =0.25, 0.33, 0.16, 0.12, 0.21. Some of them, e.g. at 0.09, 0.12 and 0.19 have a "split" form which is typical for synchrobetatron resonances. Classification of the resonances in Fig.5 accordingly to formulae of $m(\nu \pm 1/4) =$ integer says that the resonances up to the order of $m = 10 - 16$ take place.

Weak resonances of high orders are usually not well seen after a small number

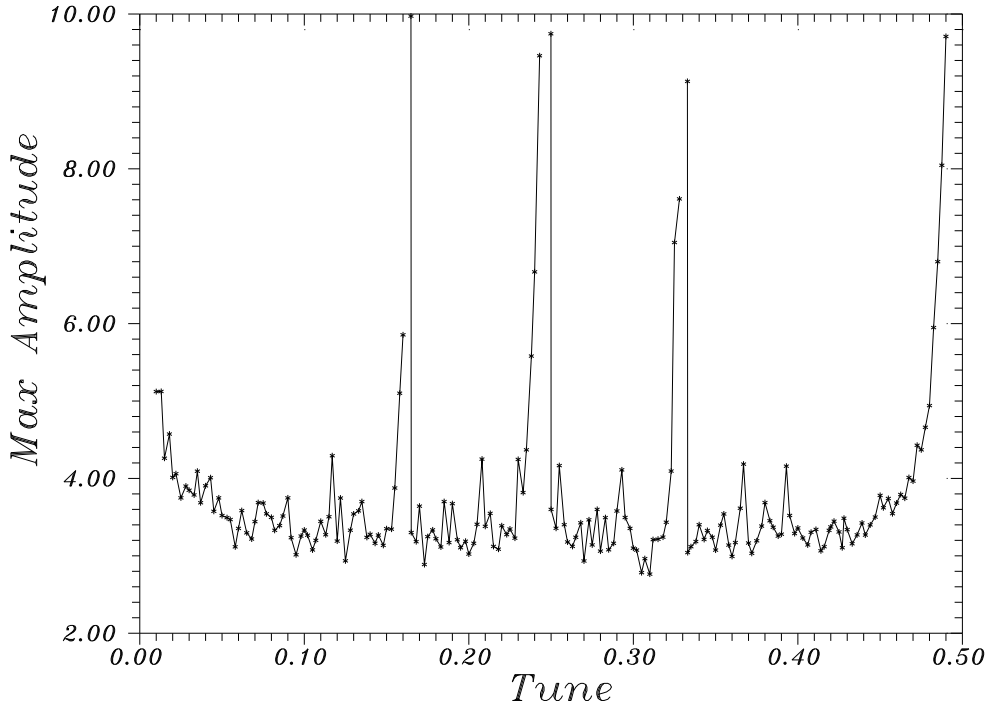


Figure 5: Maximum betatron amplitude $A_{max}/\sigma_0$ vs betatron tune $\nu_y = \nu_x = nu$ for the Mobius scheme with $\xi = 0.05$ (100,000 turns).

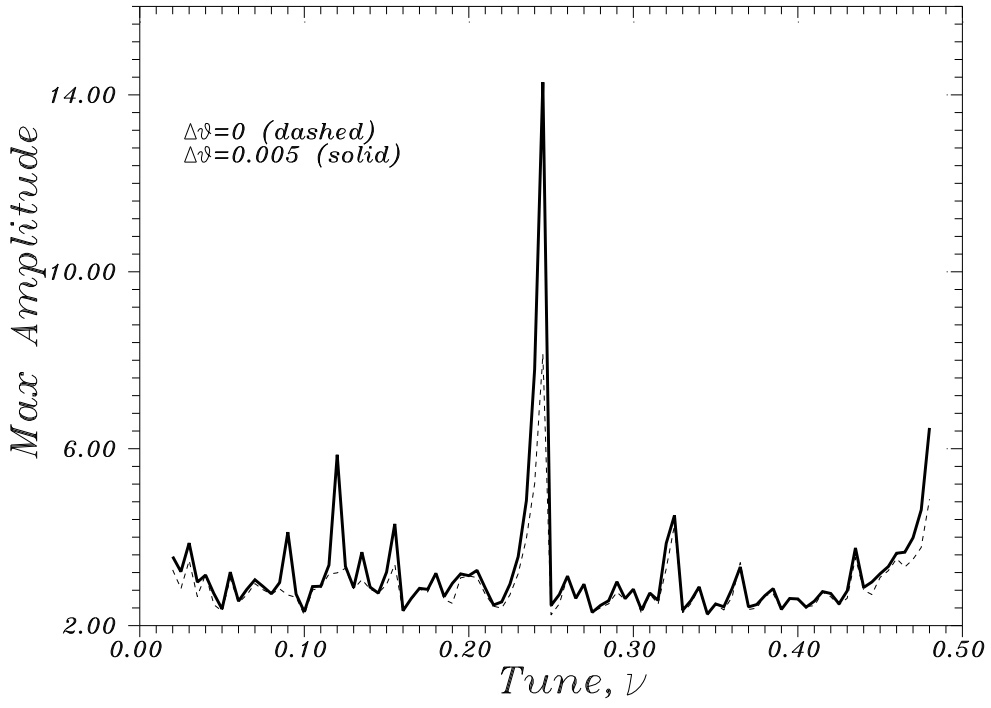


Figure 6: Maximum betatron amplitude $A_{max}/\sigma_0$ vs betatron tune $\nu_y = \nu_x = nu$ for the Mobius scheme with and without betatron betaron tune variation of $\Delta\vartheta = 0.005$. 75,000 turns, $\xi = 0.05$.

of revolutions and in order to enhance them we used a method of the Ornstein-Uhlenbeck tune modulation, developed in [22]. The Ornstein-Uhlenbeck process is "random-walk" like changes in the betatron phases which are added to the phase advances in the arcs of $\mu_{x,y} = 2\pi\nu_{x,y}$ at every turn:

$$\Delta\mu_{x,y}^{new} = (1 - \frac{1}{N_c})\Delta\mu_{x,y}^{old} + \Delta\vartheta\sqrt{\frac{2}{N_c}}\zeta_{x,y}^{new}, \tag{52}$$

where $\Delta\vartheta$ is the rms value of the phase modulation (corresponding tune modulation is equal to $\Delta\nu_{x,y\,rms} = \Delta\vartheta/2\pi$), $N_c$ is the characteristic number of turns over which the modulation is partially correlated (typically we used $N_c = 100$ turns), and $\zeta_{x,y}$ are two independent sets of random numbers with zero mean value and the variance of 1.0. The mean values of $\Delta\mu_{x,y}$ are equal to 0. Such tune modulation enhances particles' flux to larger amplitudes, emphasize resonances, but, having a continuous spectrum, it does not create new resonances [22] [7].

Fig.6 demonstrates how the phase modulation of $\vartheta = 0.005$ some resonances in the tune scan of the Mobius scheme "head-on" collisions. One can see that with respect to no-modulation case the maximum betatron amplitudes at $\nu$ =0.09, 0.11, 0.13, 0.16 are grown up to values of 6-8 after only 75,000 turns while after 100,000 turns in previous Fig.5 all they were less or about 4. (Note, that the step size of $\nu$ is 0.0025 in Fig.5 and twice larger in Fig.6).

Now, with use of smaller phase modulation of $\vartheta = 0.002$, we compare the rms beam sizes after 50,000 turns for the round beams and the beams which are far from round. The colliding round beams (without any coupling, or in $R(0)$ scheme) satisfy to all the conditions:
$\varepsilon_x = \varepsilon_y = 3 \cdot 10^{-9}$ m$\cdot$ rad;
$\beta_x^* = \beta_y^* = 25$ cm;
$\nu_x = \nu_y = \nu$,
while the "not-RBs" break them all:
$\varepsilon_x = 5/3\varepsilon_y = 5 \cdot 10^{-9}$ m$\cdot$ rad;
$\beta_x^* = 35/25\beta_y^* = 35$ cm;
$\nu_x = \nu\ \nu_y = \nu + 0.18 \neq \nu_x$.
As the result, the maximum $X, Y$ betatron amplitudes (see Fig.7) for the non-round beams are larger than the amplitude at the RBs case. Several strong resonances are seen in the non-RB curves while the RBs perform only the size increase at $\nu = 0.25$.

## 4.4 Simulations with "inverse beta function" charge distribution. Optimum bunch length.

As it was pointed out in the previous Section, the beam-beam interaction of the bunches with the "inverse beta function" longitudinal charge distribution can provide

[7] with periodic tune modulation, additional resonances at combined frequencies appear and, thus, fakes the natural resonance set.

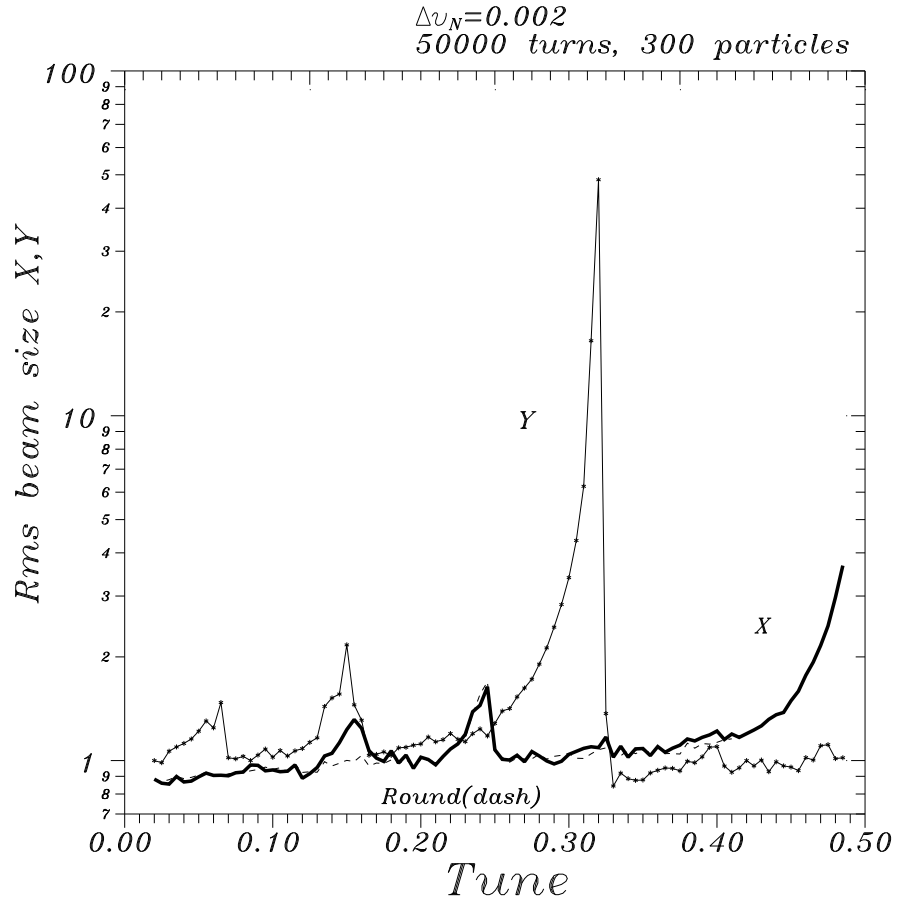


Figure 7: The rms beam size $\sigma/\sigma_0$ vs betatron tune $\nu_y = \nu_x = nu$ for the Mobius scheme (dashed line), and the rms horizontal and vertical sizes $\sigma_{x,y}/\sigma_{0\,x,y}$ for non-round beams (solid and marked lines, respectively). ($\xi$ = 0.05, = 0.002, 50,000 turns).

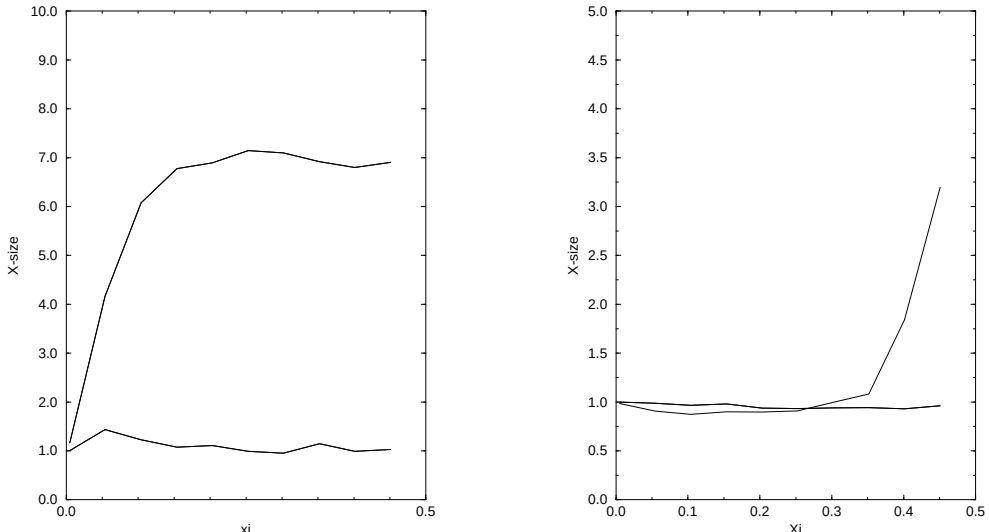


Figure 8: Beam size after 50,000 turns versus $\xi$. The upper curve corresponds to the short strong Gaussian bunch, the lower one — to the strong counter bunch with the "inverse beta-function" distribution. The beta-function at IP is 25 cm. **a** – left figure – tunes are equal to $\nu_x = \nu_y = -0.01$; **b** – right figure – tunes are equal to 0.05.

integrable dynamics and better stability. We compare the behavior of such beams with the case of short round Gaussian colliding bunches at two working points. Note, that transverse sizes, bunch intensities, the weak bunch length of 15 cm and $\beta^* = 25$ cm are the same in both cases. Fig.8a presents the beam size growth vs. $\xi$ after 50,000 turns for $\nu = -0.01$.

From the upper curve one can see significant growth of the beam sizes of the short bunches with increase of $\xi$, while there is almost no effect for the integrable case (in fact, we allowed about 10% deviation of the longitudinal charge distribution in the strong bunch from the exact $1/\beta(s)$ solution) – see the lower curve. There is only a small growth at $\xi \simeq 0.1$; if the charge distribution differs on about 1% from $1/\beta(s)$ then there are no peaks at all and the beam size is not changing in time (this trivial result is not presented).

The second working point of $\nu = 0.05$ looks better for the both cases and Fig.8b shows a significant difference between the two cases only for large $\xi$.

If it's difficult to make such a distribution function, one can choose the best ratio of the length of the Gaussian bunch and beta-function at IP (the previous results for the Gaussian bunch were obtained with a very short strong beam). This optimum length depends on the working point. For better understanding of this fact, we use a simple model of the "flat-top" (or rectangular) charge distribution over the full length of $l$. In Fig.9 one can see a simple scheme of a collider with 2 IPs. Let's assume, that the beta function is almost constant over the bunch length $\beta(s) \approx \beta_0$ and the longitudinal distribution is a constant within the coordinate interval of $\pm l/2$ and vanishes elsewhere (as well as the transverse kick). If in between of the tail of one bunch and the head of another we have the unity transformation $I$ of the betatron variables (or minus unity $-I$ – here it doesn't matter, as the potential of the round beam is symmetrical function of coordinates), then one can leave out the arcs and connect kicks from all our bunches together as the bottom line of boxes shows in Fig.9. As here is no dependence of the force on time so this dynamical system is integrable and has no resonances. If the phase advance in the arcs $\Delta\nu$ is non exactly zero, then one gets overlapping of forces for the negative phase advance, or interruptions in the force for the positive one. Time modulation of the force leads to unwanted resonances, therefore, the case with the unity matrix in the arcs is an optimum.

To keep the condition, the total phase advance over half a turn has to be equal to the latter over the bunch length:

$$d\psi = ds/\beta_0 = l/2\beta_0, \tag{53}$$

where the factor 1/2 appears from the double relative speed of the test particle and counter beam. So this relation sets the optimum bunch length as a function of $\beta_0$, or optimum (fractional) tune in the arcs $\Delta\nu = \frac{d\psi}{2\pi}$.

For the Gaussian bunch such a simple estimate is no more valid, nevertheless, our simulation near integer and half-integer tunes, shows approximately the same relation of the beta function at IP $\beta^*$, tune $\nu$ and the bunch length as the one presented above.

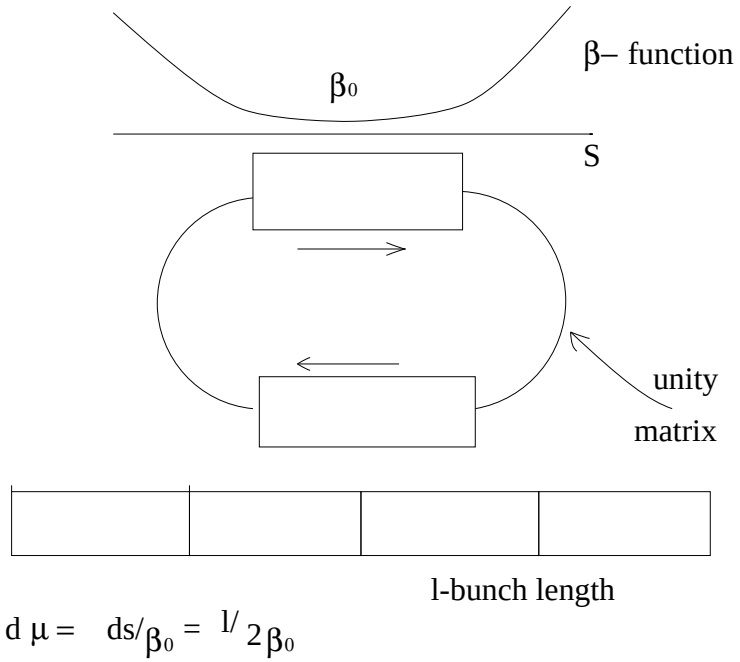


Figure 9: Scheme of collider for the flat-top longitudinal distribution of counter beam.

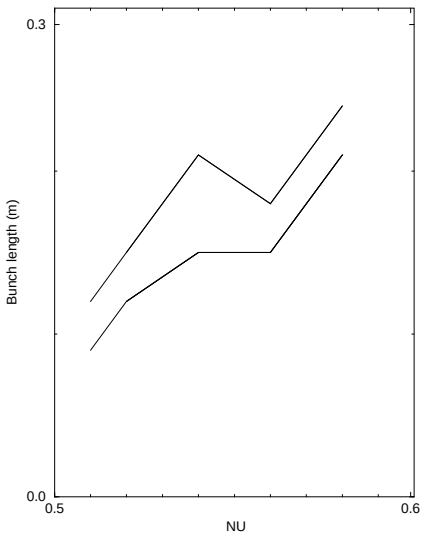


Figure 10: Bunch length of strong beam versus tune for the optimum beam lifetime (the upper curve) and for the smallest beam size growth (the lower curve) near the half-integer resonance.

For example, two curves in Fig.10 presents the optimum rms bunch length $\sigma_s$ vs. tune $\nu$ for the maximum lifetime (upper curve) for the slowest beam size growth (lower curve, $\beta^*$=25 cm, 30,000 turns, $\xi = 0.8$) [8]. Both optimum curves are close to the analog of Eq.(53) $\sigma_s^{optimum} \propto 2\pi\beta^*(\nu - 0.5)$. There exist other favorable relations of tune and length in the full area of these parameters.

We performed a search for optimal $\sigma_s$ over tunes of $\nu_x = \nu_y = \nu = 0.02...0.25$ – see Fig.11 with the contour plot of the maximum betatron amplitude $A/\sigma_0$ in the "no-coupling" RB variant vs. $\sigma_s$ and $\nu$ (75, 000 turns, $\xi$ =0.05, $\beta^* = 25$ cm, phase modulation of $\vartheta = 0.002$). The optimal bunch length (at which, say, $A/\sigma_0 \simeq 4$) depends on the tune and is about 30 cm for the tune around 0.2, about 20 cm for the tune around 0.12, and about 40 cm for the area of a good lifetime near the integer resonance. The last one corresponds to formula $\sigma \simeq \sqrt{2}\beta^*$. One of the probable explanation of that relation can be that the first terms in Tailor expansion of the Gaussian distribution $f(s) \propto \exp -s^2/2\sigma_s^2$ and the "inverse beta function" distribution $f(s) \propto 1/(1 + (s/2\beta^*)^2)$ are equal if $\sigma_s = \sqrt{2}\beta^*$. It is interesting to note, that similar results on the optimum bunch length were observed in beam-beam simulations of the RCBs in electron-positron colliders [5].

## 4.5 Beams separation effects

Separation of beams at the IP leads to geometrical luminosity reduction as well as to stronger nonlinearities of the beam-beam forces for larger number of particles. Broken symmetry of the interaction results in appearance of new (odd order) resonances worsening the collider performance. The closed orbit looks different for the three schemes of the round beams operation. For the uncoupled accelerator it is easy to find a new orbit by means of usual 1-D formulas. For the Möbius scheme, a dipole kick of $\vec{k} = (0, k_x, 0, k_y)$ causes the distortion of the closed orbit

$$\vec{\Delta} = C \cdot \vec{k},$$

where the matrix $C$ is equal to:

$$T = (I - M)^{-1} = \begin{pmatrix} I & -T_y \\ T_x & I \end{pmatrix}^{-1} \tag{54}$$

$I$ is the $2 \times 2$ identity matrix and $T_{x,y}$ is defined in Eq.(49).

After some algebra we have:

$$T = \begin{pmatrix} A & B \\ -B^T & A \end{pmatrix}, \tag{55}$$

[8] for every value of tune $\nu$ we found optimum(minimum) in maximum amplitude – lifetime indicator, or in the rms size growth by scanning the length, and that is shown in Fig.10

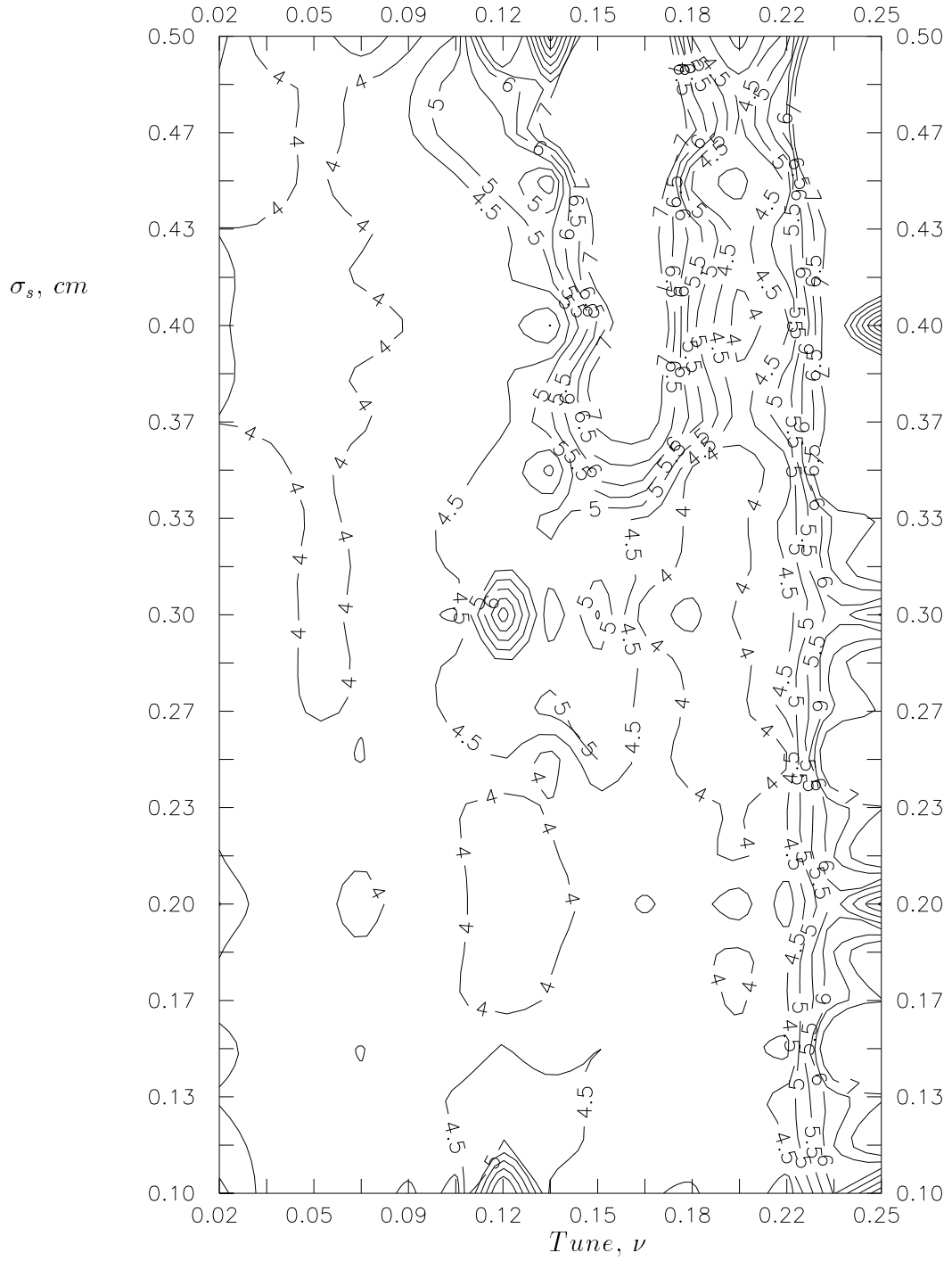


Figure 11: Contour plot of maximum betatron amplitude $A_{max}/\sigma_0$ vs rms bunch length $\sigma_s$ and tune $\nu_y = \nu_x = nu$. '$R(0)$ scheme of the "round beams", $\xi = 0.05$, $\Delta\vartheta = 0.002$, 75,000 turns.

where $^T$ means transposition and $A, B$ are:

$$A = \begin{pmatrix} \frac{1}{2} & -\frac{1}{2}\tan(\frac{\mu_x+\mu_y}{2}) \\ \frac{1}{2}\tan(\frac{\mu_x+\mu_y}{2}) & \frac{1}{2} \end{pmatrix}, B = \begin{pmatrix} \frac{1}{2}\frac{\cos(\frac{\mu_x-\mu_y}{2})}{\cos(\frac{\mu_x+\mu_y}{2})} & -\frac{1}{2}\frac{\sin(\frac{\mu_x-\mu_y}{2})}{\cos(\frac{\mu_x+\mu_y}{2})} \\ \frac{1}{2}\frac{\sin(\frac{\mu_x-\mu_y}{2})}{\cos(\frac{\mu_x+\mu_y}{2})} & \frac{1}{2}\frac{\cos(\frac{\mu_x-\mu_y}{2})}{\cos(\frac{\mu_x+\mu_y}{2})} \end{pmatrix}.$$

These expressions were inserted in the code for determination of the new orbit at the IP, as well as expressions for the "back-and-forth" rotation (the corresponding formula for the last case can be derived in the same manner).

Results of the simulations of the maximum betatron amplitude, the rms beam size and the luminosity reduction under condition of about 1 sigma separation in both planes $\Delta X = \Delta Y = 30\,\mu$m are presented in Fig.12a,b,c, respectively. First of all, one can see that after only 75, 00 turns the maximum betatron amplitudes can reach the values up to 80 initial rms sizes $\sigma_0$. The resonances are stronger and more numerous for the Mobius scheme, and they are least visible in the no-coupling option. The same preference of no-coupling is true for the beam size and luminosity. We'd like to note that higher luminosity and smaller maximum amplitudes take place for small tunes $\nu \leq 0.08$.

## 4.6 Crossing angle at the IP

The effects of the crossing angle at the interaction points of the Tevatron is studied in Ref.[23]. Besides purely geometrical luminosity reduction, detrimental manifestation of the synchrobetatron resonances is found to be a source of troubles for the collider with the normalized angle of $\Phi = \phi\sigma_s/\sigma_x \geq 1$. These resonances enhance the particles diffusion to large amplitudes and reduce the tune area available for a good machine operation. The effect grows at larger $\xi$. Here we present the RCBs simulation with the crossing angle.

Fig.13 presents the maximum betatron amplitude after 50,000 turns with the crossing angle of 0.1 mrad $\Phi \simeq 0.5$ (solid curve), and without the angle (dashed curve) vs. the tune $\nu = \nu_x = \nu_y$. The diagonal tune scan is to fulfill the condition of the RCBs without coupling. One can see that, first of all, several new resonances appear at $\nu$ =0.19, 0.21, 0.29, 0.35, 0.37, 0.39, 0.42; then, even in between the major resonances there is significant increase of the amplitude due to the angle. Nevertheless, not-round beams show much worse performance with the crossing angle (see Fig.14, note the enlarged scale with respect to previous Figure), and drastic diffusion growth covers almost the whole tune space.

To study which of the RCBs schemes shows better performance with the crossing angle of $\phi = 0.2$ mrad ($\Phi \simeq 1$, about the TeV'33 design value) we perform a scan of the maximum betatron amplitude vs. the tune $\nu$ and the nominal beam-beam parameter $\xi$. The resulted contour plots are shown in Figs.15,16,17 for $R(0)$, $R(\pm\pi/2)$ and $R(\pi/2)$ schemes, respectively. One can see that the area of $\nu - \xi$ parameters with comparatively small value of $A_{max}/\sigma_0 \leq 4...5$ is the largest for the "no-coupling"

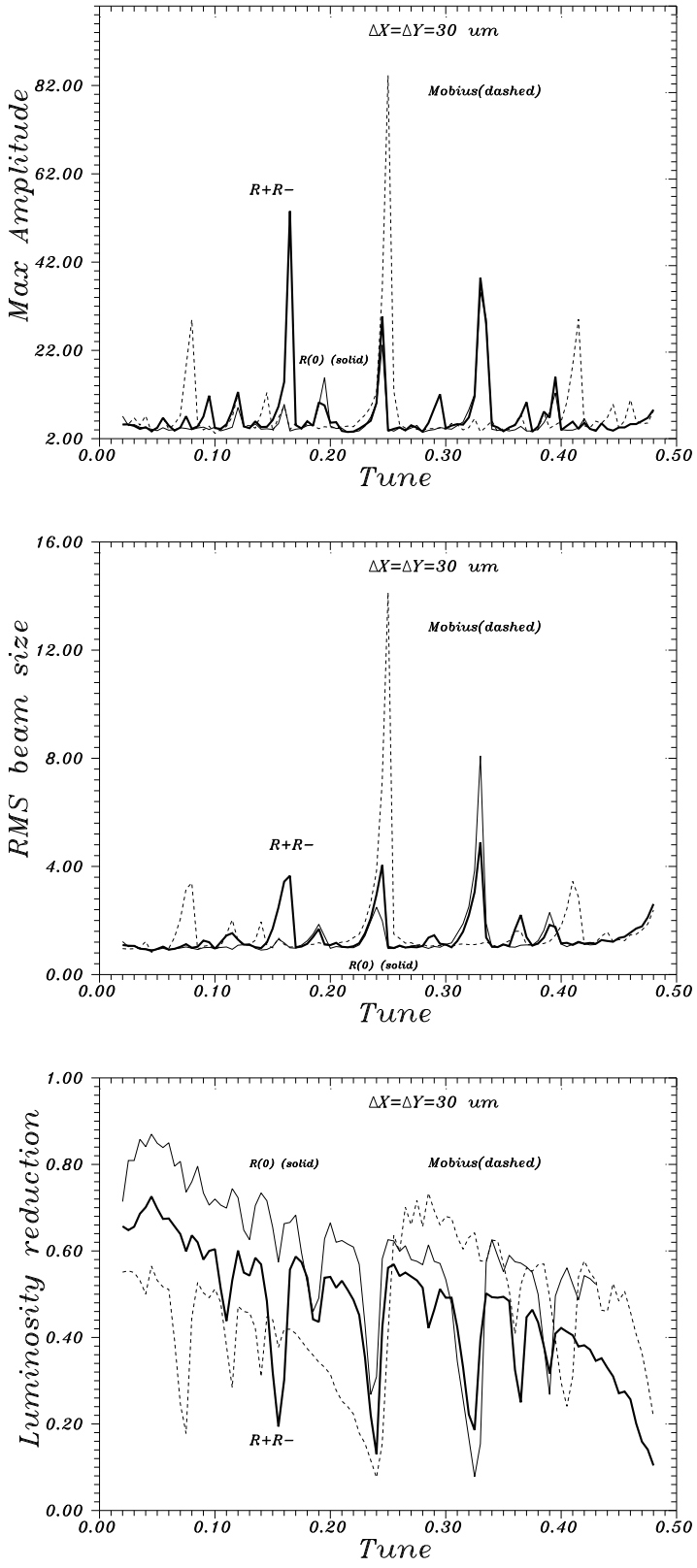


Figure 12: Effects of separation $\Delta X = \Delta Y = 30\,\mu\text{m} \approx 1\sigma_0$. **a**(top) – maximum betatron amplitude vs. $\nu$; **b**(center) – the rms beam size vs. $\nu$; **c**(bottom) – the luminosity reduction factor vs. $\nu$. Everywhere the "no-coupling" RCBs scheme is marked by thin solid line, the Mobius scheme – by dashed line, the $R(\pm\pi/2)$ scheme – by thick solid line. $\xi = 0.05$, $\Delta\vartheta = 0.005$, 75,000 turns.

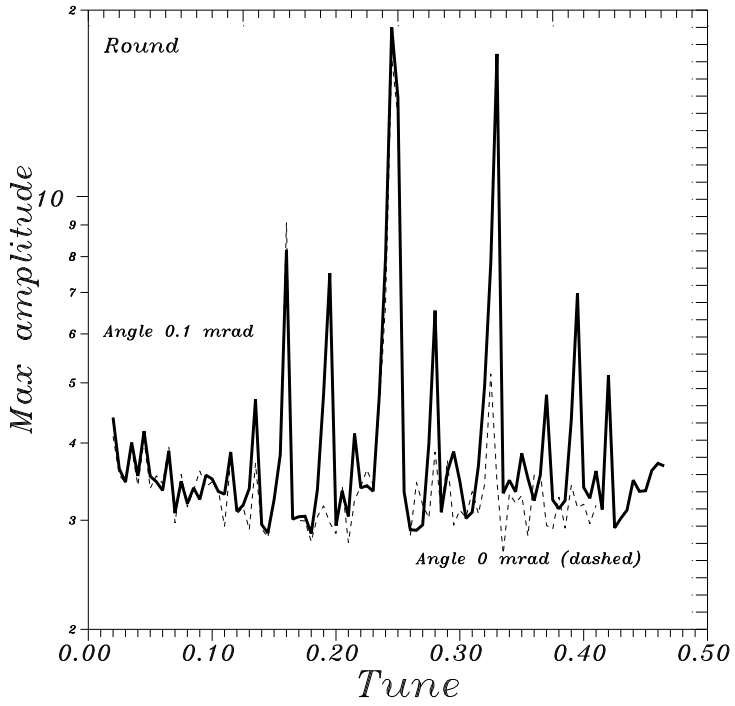


Figure 13: Maximum betatron amplitude with and without 0.1 mrad crossing angle at the IP (solid and dashed lines, respectively). "No-coupling" scheme of the "round beams" with $\xi = 0.05$, $\Delta\vartheta = 0.002$, 50,000 turns.

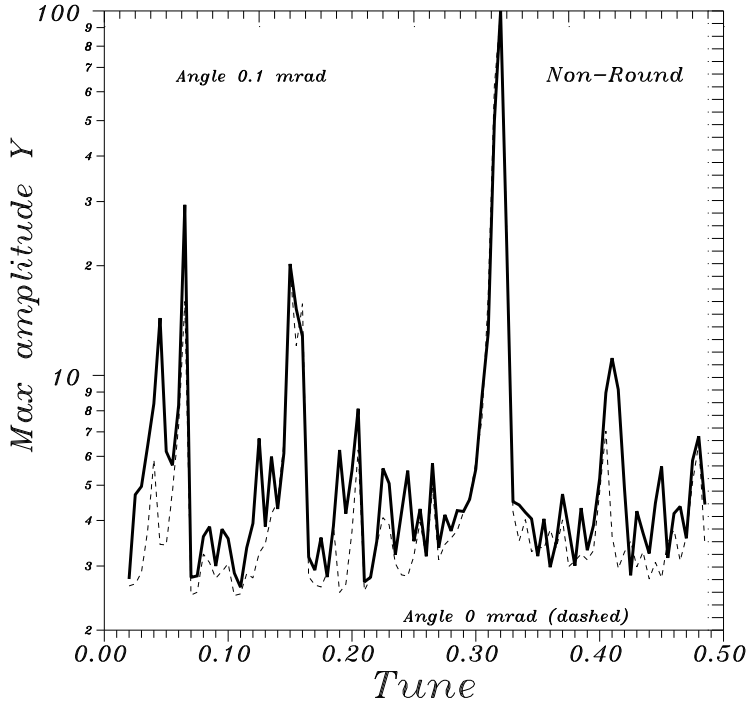


Figure 14: Maximum vertical betatron amplitude with and without 0.1 mrad crossing angle at the IP (solid and dashed lines, respectively). The "round beams" conditions are not fulfilled. $\xi = 0.05$, $\Delta\vartheta = 0.002$, 50,000 turns.

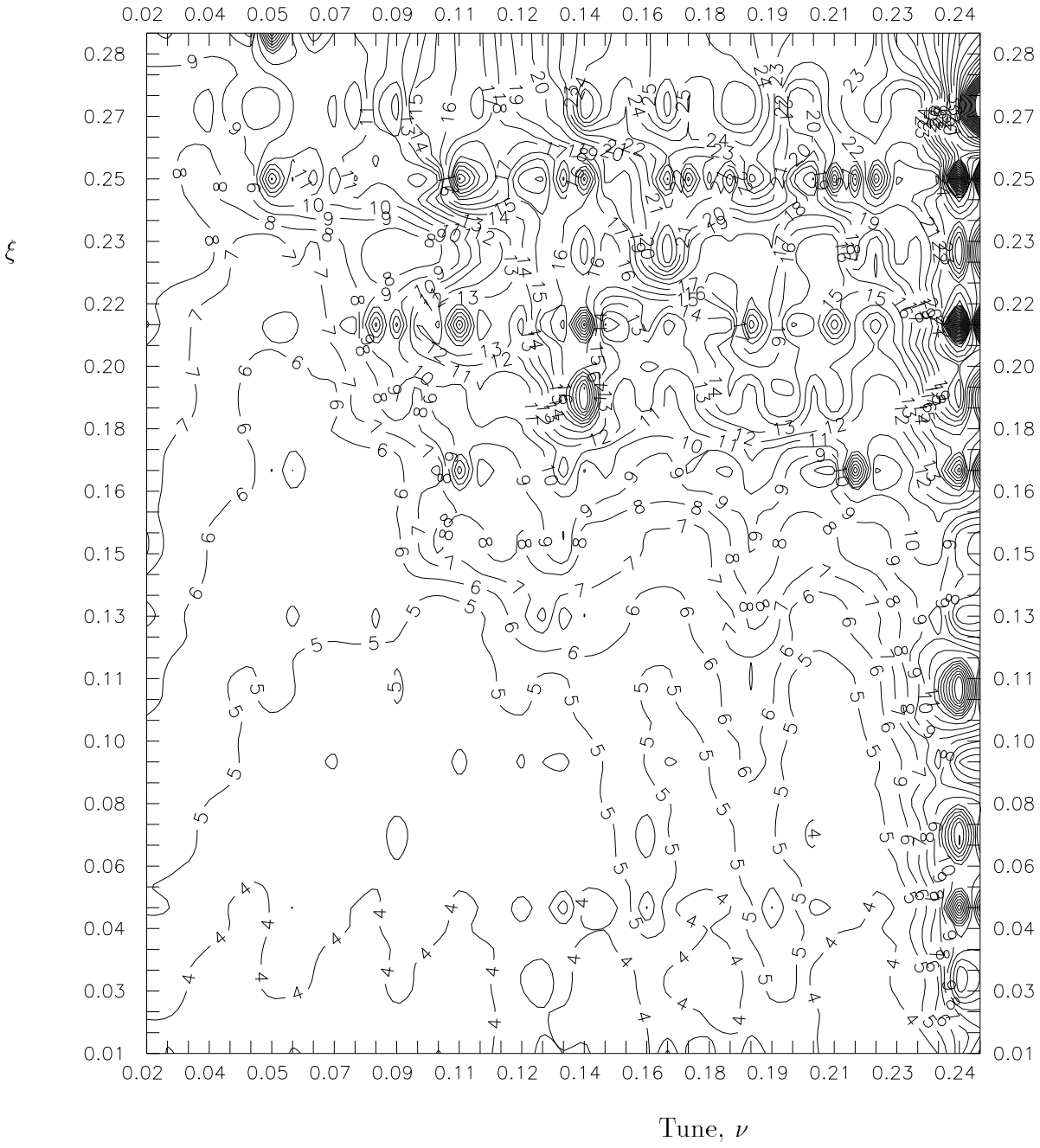


Figure 15: Contour plot of the maximum betatron amplitude after 100,000 collisions of the round beams, "no-coupling" scheme, with 0.2 mrad crossing angle (normalized angle of $\Phi \simeq 1$) versus the beam-beam parameter $\xi$ and the tune $\nu_x = \nu_y = \nu$. $\Delta\vartheta = 0.002$.

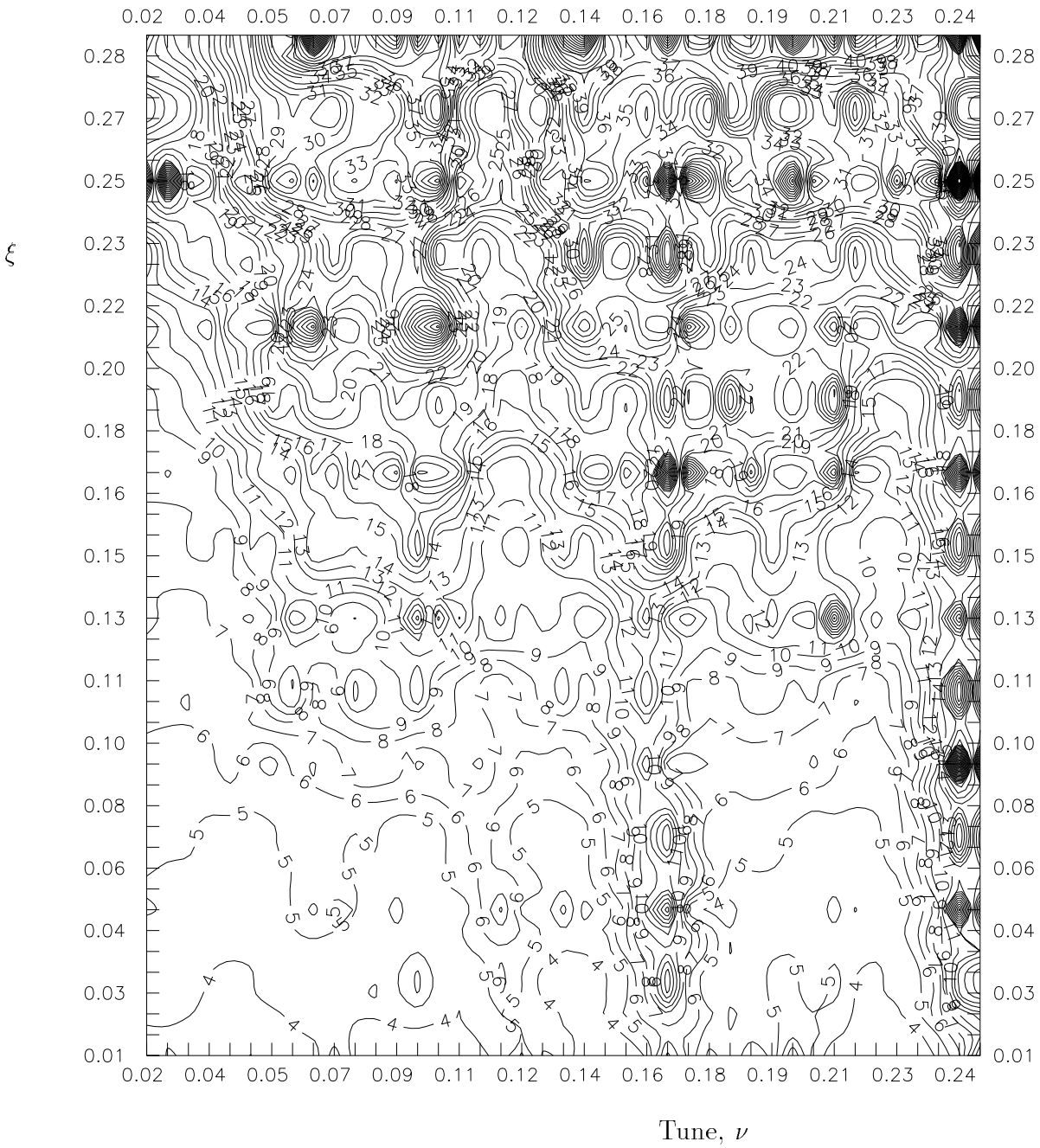


Figure 16: The same as in Fig.15 but for "back-and-forth" option of "round beams".

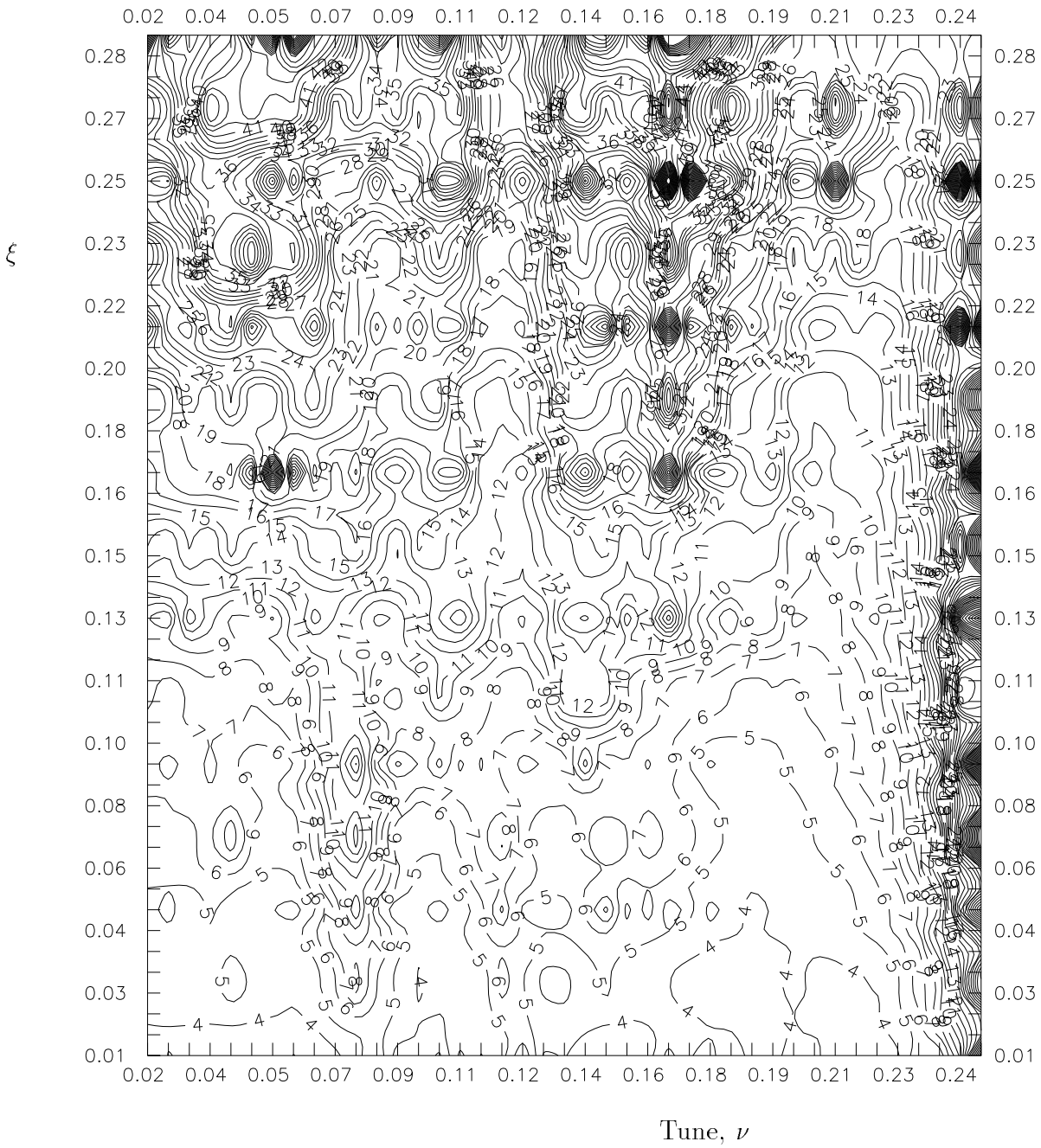


Figure 17: The same as in Fig.15 but for Möbius option of "round beams".

option and the smallest for the Mobius one. One can conclude that less coupling is better from point of view of the synchrobetatron effects.

## 4.7 Effects of the dispersion at the IP

The next source of the machine imperfections we investigate for the RCBs is the (residual) dispersion at the IP. It is known to lead to coupling between synchrotron and betatron oscillations. Indeed, the transverse displacement of the orbit for the off-momentum particle is $\Delta x = \eta_x(\delta p/p)$ where $\eta_x$ is the dispersion function, and $(\delta p/p)$ is the relative particle momentum deviation. The beam-beam kick depends on $x$, therefore, if $\eta \neq 0$ then the interdependence of the longitudinal momentum deviation and the transverse oscillation takes place.

The consequences are shown in Fig.18 which present the maximum betatron amplitude after 75,000 turns in the $R(0)$ machine without the dispersion (dashed line) and with $\eta_x = \eta_y = 2$ cm at the IP. One can clearly see appearance of the resonances at the tunes of 0.19, 0.27, 0.36 and 0.39, and significant increase of the diffusion at previously existing resonances at $\nu$=0.16, 0.25, 0.33. The next Fig.19 compares three RCB schemes (thick solid line is for "no-coupling" RCBs, dashed – for "back-and-forth coupling" or $R(\pm\pi/2)$, and thin solid line is for Mobius collider), and one again can conclude that "no-coupling" case is the best of three as there are smaller $A_{max}$ and weaker resonances. We intentionally take here comparatively large dispersion of $\eta = 2$ cm (the effective size due to dispersion $\sigma_{disp} = \sqrt{\eta_x^2 + \eta_y^2} \cdot (\Delta E/E) \simeq 62\,\mu$m, that is more than twice the betatron size of $\sqrt{\beta^* \varepsilon} \simeq 28\,\mu$m) in order to emphasize the effect.

## 4.8 Asymmetry between two IPs

The degradation of the collider performance due to beam-beam effects are often thought to be more significant if there are several asymmetric interaction points. Fig.20 and Fig.21 present results of the maximum amplitude simulations for the $R(0)$ and the Mobius collider correspondingly with two IPs. If one denotes the phase advance between the first IP and the second one as $\nu$ and between the second one and the first one as $\nu + \Delta\nu_{1,2}$ then the horizontal axis is for $\nu$ and the vertical axis is for $\Delta\nu_{12}$. The lighter areas correspond to smaller maximum betatron amplitude after 10,000 turns, the contour spacing goes as follow: $(A_{max}/\sigma_0)$=4, 5, 7, 10, 15, 20, 25, 30, 40, 50.

One can see that for $\Delta\nu_{12} \neq 0$, there are larger white areas with small $A_{max}$ in the "no-coupling" case than for the Mobius collisions. It is interesting to note, that over large tune space the optimum in $A_{max}$ for the both schemes lays out of the condition of symmetry, i.e. at $\Delta\nu_{12} \neq 0$.

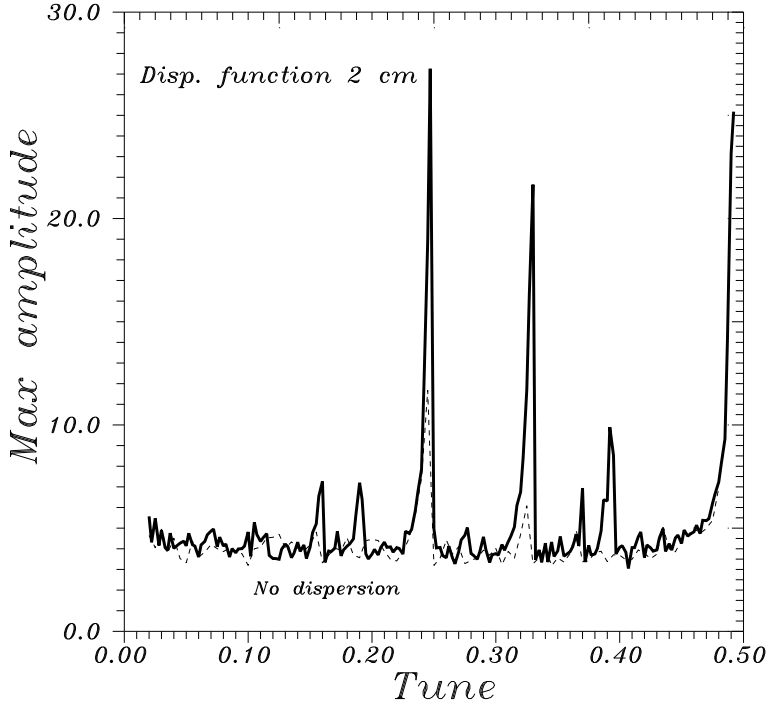


Figure 18: Maximum betatron amplitude with and without dispersion of $\eta_x = \eta_y = 2$ cm at the IP (solid and dashed lines, respectively). "No-coupling" scheme of the "round beams" with $\xi = 0.05$, $\Delta\vartheta = 0.002$, 75,000 turns.

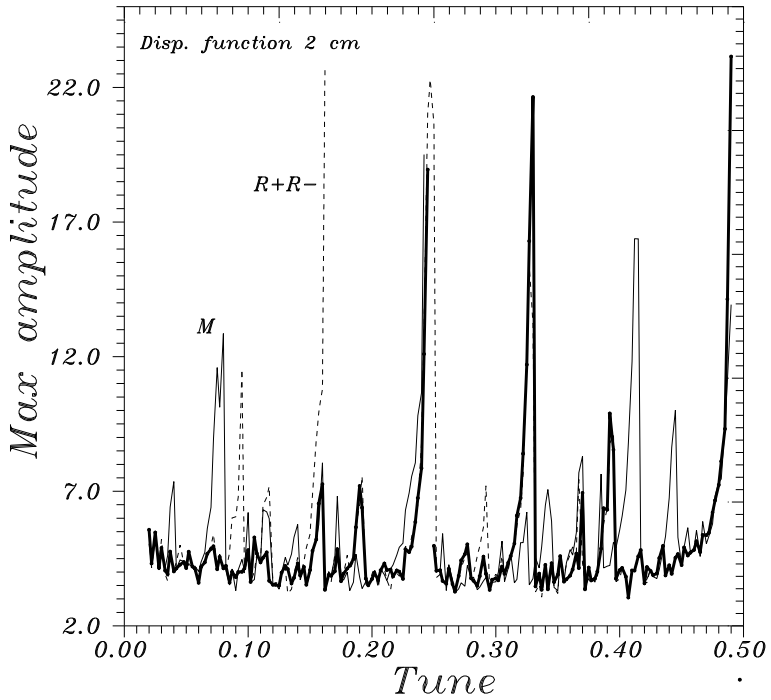


Figure 19: Maximum betatron amplitude without dispersion of $\eta_x = \eta_y = 2$ cm at the IP for three options of the "round beams"(thick solid line – for $R(0)$, dashed line – for $R(\pm\pi/2)$, thin solid line – for $R(\pi/2)$). $\xi = 0.05$, $\Delta\vartheta = 0.002$, 75,000 turns.

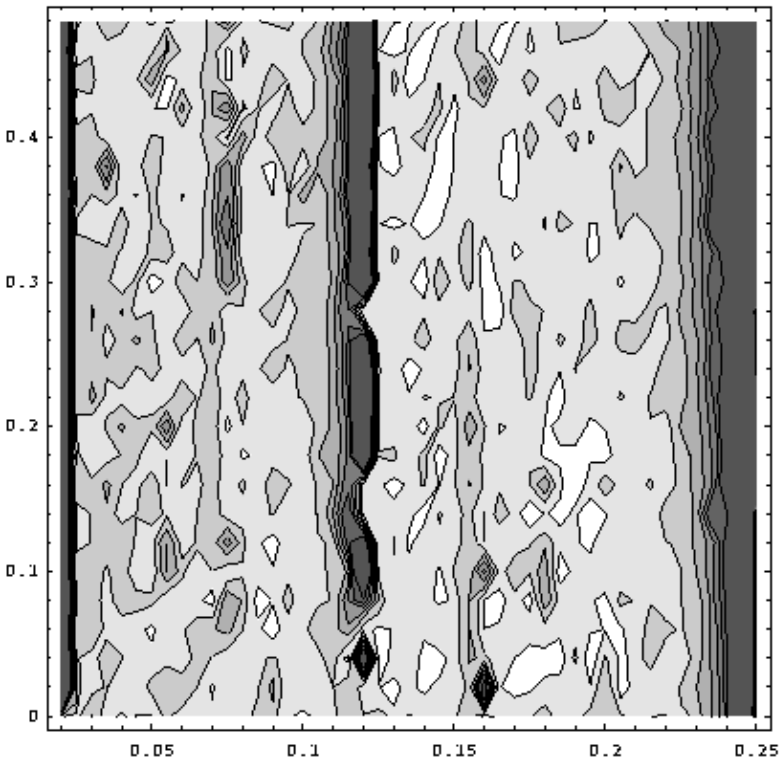


Figure 20: Contour plot of the maximum betatron amplitude vs. tune $\nu$ (horizontal axis and the tune difference between two IPs $\Delta\nu_{12}$ (vertical axis) for the "not-coupled" round beams. $\Delta\vartheta = 0.002$, 100,000 turns.

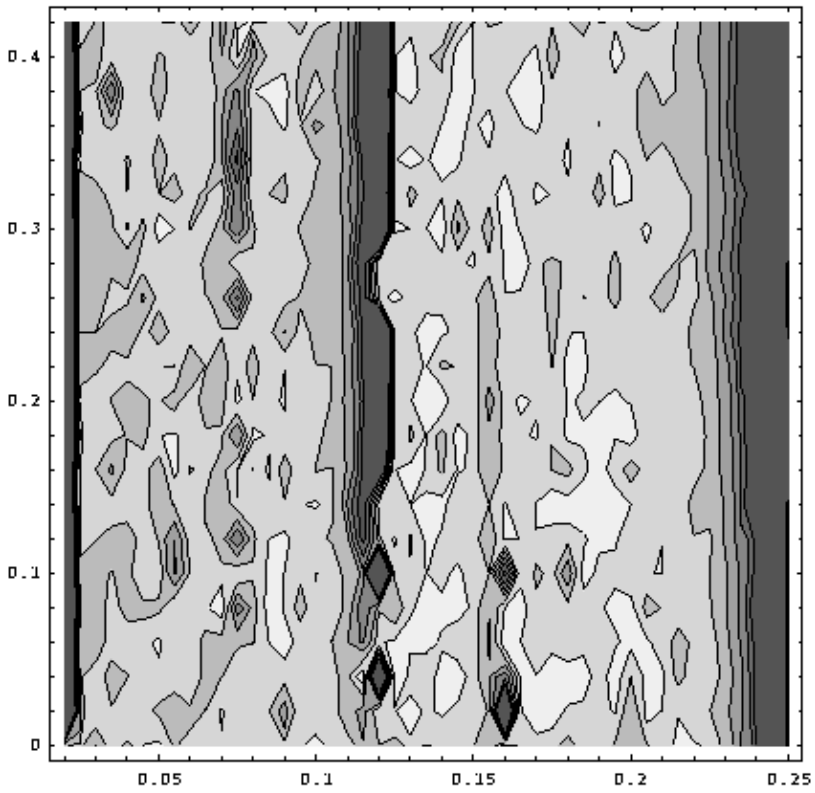


Figure 21: Contour plot of the maximum betatron amplitude vs. tune $\nu$ (horizontal axis) and tune difference between two IPs $\Delta\nu_{12}$ (vertical axis) for the Mobius beams. $\Delta\vartheta = 0.002$, 100,000 turns.

# 5 Conclusion

In this article we studied new ways to improve single particle stability in colliders. The essence of these ways is obtaining integrability of the particles' dynamics with proving additional integrals of the particle motion. For example, if the "round beams" conditions are fulfilled, then the longitudinal component of the angular momentum is the invariant for colliding beams. Further studies have shown that choosing the longitudinal charge distribution of the strong bunch close to the "inverse beta function" one can eliminate all beam-beam resonances at all. Another suggested example with some specific transverse bunch charge distribution (although close to a natural one) leads to existence of additional (to the angular momentum) integral of motion which is quadratic in momentum. We performed also a general investigation of accelerator-like dynamical systems with invariants polynomial in momentum.

The presented integrable systems with only regular motion and without beam-beam blow-up threshold have strengthened the concept of round colliding beams. The beam emittance growth becomes mostly determined by the focusing lattice nonlinearities and imperfections, so we believe that it will be possible to achieve a higher luminosity by reducing the impact of nonlinear resonances.

The second part of the work is devoted to simulations of the round beams. We described three schemes of the RBs realization ("no $x$-$y$ coupling" or $R(0)$ scheme, the Mobius accelerator or $R(\pi/2)$, and the "back and forth" coupling scheme or $R(\pm\pi/2)$). Note, that in the absence of any cooling, hadron beams are naturally round in geometrical sense, while in electron-positron storage rings some coupling is necessary to obtain the RCBs. The BBC code was used to simulate collisions in the Tevatron $p\bar{p}$ collider, track test particles and study dependencies of the maximum betatron amplitudes, the rms beam sizes and the luminosity reduction factors on various beam imperfections. From the simulations we conclude that in the presence of the beam-beam interaction, the round beams show better particle stability and slower transverse diffusion rates than not-round beams, they also are more stable with respect to various errors and noises (e.g. tune variation). Among the three RCBs options, the "no-coupling" one is found to be the most tolerant to the disturbances like the crossing angle at the collision point, the beam-beam separation, residual dispersion at the IP, asymmetry between two IPs. We also performed a search for optimum bunch length and found a qualitative agreement with our analytical studies of the RCBs.

The model we used in our simulations is not quite adequate to the Tevatron, first of all because of limited prediction ability of the "weak-strong model", and then, because of rather simplified presentation of the machine lattice besides the interaction region: we do not take into account nonlinear field components, residual $x - y$ coupling, and other imperfections at the arcs. We track particles over comparatively small number of turns $N_{turns} \leq 300{,}000$ because of CPU time limitations. Simple check has shown that under far off resonant conditions, the calculated luminosity and beam

sizes almost don't depend on $N_{turns}$, while the maximum betatron amplitudes grow very slowly with $N_{turns}$. In order to enhance the appearance of some subtle dynamical effect we often used either larger interaction parameter $\xi$ or introduced tiny "random walk"-like tune variation of the lattice.

Possible topics for further studies can be effects of non-linearities outside the IP, consequences of the RCBs implementation for intrabeam scattering issues and for the effects of the parasitic interactions.

## Acknowledgments

Authors thank K. Hirata(KEK) for an opportunity to use his simulation code and his helpful advises concerning its operation. We sincerely acknowledge numerous and fruitful discussions with E. Perevedentsev, I. Nesterenko, D. Shatilov, Yu. Shatunov and P. Ivanov (Novosibirsk INP), P. Bagley, J. Marriner, D. Finley and L. Michelotti (FNAL), R. Talman and E. Young (Cornell), Ya. Derbenev (Michigan University, Ann-Arbor) and J. Cary (University of Colorado, Boulder). We are thankful to E. Perevedentsev for careful reading the manuscript and numerous corrections.

# References

[1] F.M. Izrailev, G.M. Tumaikin, I.B. Vasserman. Preprint INP 79-74, Novosibirsk (1979).

[2] A.G. Ruggiero, "Integrability of the Two-Dimensional Beam-Beam Interaction in a Special Case", *Particle Accelerators*, v.12 (1982), p.45.

[3] T. Bountis, C.R. Eminhizer, and R.H.G. Helleman, in *Long-time Prediction in Dynamics*, eds., W.Horton, L.Reichl, and V.Szebehely, (J.Wiley, NY, 1982).

[4] L.M. Barkov, *et. al, Proc. 14th Int. Conf. High Energy Accelerators*, Tsukuba, Japan (1989), p.1385.

[5] S. Krishnagopal, R. Siemann, "Simulations of Round Beams", *Proc. of 1989 IEEE PAC,* Chicago (1989), p.836.

[6] *Proc. of III Advanced ICFA Beam Dynamics Workshop on Beam-Beam Effects in Circular Colliders*, I. Koop and G. Tumaikin, Eds., Novosibirsk (1989).

[7] V.V.Danilov *et. al, Proc. 1991 IEEE PAC*, San Francisco (1991), p.526.

[8] A.N. Filippov *et. al, Proc. 15th Int. Conf. High Energy Accelerators*, Hamburg (1992), p.1145.

[9] Ya. Derbenev, "Invariant Colliding Beams: A Concept for High Luminosity. 4. Hollow Beams: Dynamic Superfocusing", UM HE 93-27, University of Michigan, Ann Arbor (1993).

[10] R. Talman, "The Mobius Accelerator", *Phys.Rev.Lett.*, v.74, N.9 (1995), p.1590.

[11] V.V.Danilov, *et. al,* "The Concept of Round Colliding Beams", *Proc. EPAC'96*, Barcelona (1996), p.1149.

[12] *Workshop on "Round Beams and Related Concepts in Beam Dynamics"*, FNAL, transparencies compiled by V. Shiltsev (December 1996);
see also V. Shiltsev, "Report on "Round Beams" Workshop", FNAL-Pub-97/005 (1997)

[13] E. Pozdeev (Novosibirsk INP), private communication.

[14] E.A. Perevedentsev, Unpublished note, Novosibirsk INP (1995).

[15] V.V. Danilov and E.A. Perevedentsev. *Proc. ICFA Workshop on Beam-Beam Effects*, Dubna, Russia (1995).

[16] V.V. Danilov and E.A. Perevedentsev, "Analytical 1D Method of Increasing the Dynamic Aperture in Storage Rings", *Proc. EPAC'96*, Barcelona (1996), p.893;
V.V. Danilov and E.A. Perevedentsev, "Integrable Nonlinear Map of the Accelerator Lattice Type", CERN SL/Note 94-21(AP).

[17] E.M. McMillan, "Some Thoughts on Stability in Nonlinear Periodic Focusing Systems", Preprint UCRL-17795, Univ. of California, Lawrence radiation Laboratory, Berkeley, California (1967).

[18] C.C. Chow and J.R. Cary, "Integrable Nonlinear Accelerator Lattices", *Phys.Rev.Lett.*, v.72 (1994), p.1196.

[19] J.P.Marriner, "The Fermilab Proton-Antiproton Collider Upgrades", FERMILAB-Conf-96/391 (1996); S.D.Holmes, *et.al*, FNAL-TM-1920 (1995).

[20] P.P.Bagley, *et.al,*, "Summary of the TeV33 Working Group", FERMILAB-Conf-96/392 (1996).

[21] K.Hirata, *Phys. Rev. Lett.,* v.74 (1995), p.2228;
K.Hirata, SLAC-Pub-6375 (1994); K.Hirata, KEK Preprint 93-190 , KEK (1993);
K.Hirata, H.Moshammer, F.Ruggiero, *Particle Accelerators*, v.40 (1993), p.205.

[22] T. Sen and J.A. Ellison, "Emittance Growth Due to Tune Fluctuations and the Beam-Beam Interaction", *Particle Accelerators*, v.55 (1996), p.[293]/47.

[23] V. Shiltsev, "On Crossing Angle at TeV'33", FNAL FN-653 (1997).